Pflügers Archiv - European Journal of Physiology (2021) 473:1339–1359
https://doi.org/10.1007/s00424-021-02546-x

INVITED REVIEW

Structural aspects of rod opsin and their implication in genetic diseases

Francesca Fanelli[1,2] · Angelo Felline[1] · Valeria Marigo[2,3]

Received: 3 January 2021 / Revised: 17 February 2021 / Accepted: 22 February 2021 / Published online: 16 March 2021

Abstract

Vision in dim-light conditions is triggered by photoactivation of rhodopsin, the visual pigment of rod photoreceptor cells. Rhodopsin is made of a protein, the G protein coupled receptor (GPCR) opsin, and the chromophore 11-*cis*-retinal. Vertebrate rod opsin is the GPCR best characterized at the atomic level of detail. Since the release of the first crystal structure 20 years ago, a huge number of structures have been released that, in combination with valuable spectroscopic determinations, unveiled most aspects of the photobleaching process. A number of spontaneous mutations of rod opsin have been found linked to vision-impairing diseases like autosomal dominant or autosomal recessive retinitis pigmentosa (adRP or arRP, respectively) and autosomal congenital stationary night blindness (adCSNB). While adCSNB is mainly caused by constitutive activation of rod opsin, RP shows more variegate determinants affecting different aspects of rod opsin function. The vast majority of missense rod opsin mutations affects folding and trafficking and is linked to adRP, an incurable disease that awaits light on its molecular structure determinants. This review article summarizes all major structural information available on vertebrate rod opsin conformational states and the insights gained so far into the structural determinants of adCSNB and adRP linked to rod opsin mutations. Strategies to design small chaperones with therapeutic potential for selected adRP rod opsin mutants will be discussed as well.

Keywords Rhodopsin · GPCRs · Conformational diseases · Molecular simulations · Protein structure networks

Introduction

Cell activity is regulated by extracellular signals that are recognized and transduced inside the cell via different classes of plasma membrane receptors [16, 122, 168]. G protein-coupled receptors (GPCRs) constitute the largest superfamily of signal transduction membrane proteins, which play a central role in many essential physiological processes including vision (reviewed in refs [14, 48, 83, 85, 122]). Vision in dim-light conditions is triggered upon photon absorption by the visual pigment rhodopsin, which is made of a protein, the GPCR opsin, and the chromophore 11-*cis*-retinal, covalently linked via Schiff base (SB) to K296 [35, 70, 111, 115]. As a GPCR, rod opsin is made of seven transmembrane (TM) α-helices (H) holding an up-down bundle architecture. The TM helices are connected by three intracellular (cytosolic) loops (I) and an equal number of extracellular loops (E) (intradiscal in the case of rod opsin) [35, 70, 111, 115]. The helix bundle begins with an intradiscal N-terminus (Nt) and ends up with a cytosolic C-terminus (Ct).

The common mechanism of signal transduction by GPCRs consists in agonist-induced promotion of allosteric interaction between the receptor and a member of α-family heterotrimeric αβγ guanine nucleotide-binding proteins or G proteins, which belong to the Ras GTPase superfamily [165]. These are specialized transducers that broadcast signals to intracellular effectors. Transducin (Gt) is the Gα protein deputed to visual phototransduction, the process in which light captured by a visual pigment molecule generates a detectable electrical response [11, 29, 30, 84].

This article is part of the special issue on Function and Dysfunction in Vertebrate Photoreceptor Cells in Pflügers Archiv—European Journal of Physiology

✉ Francesca Fanelli
fanelli@unimo.it

[1] Department of Life Sciences, University of Modena and Reggio Emilia, via Campi 103, 41125 Modena, Italy

[2] Center for Neuroscience and Neurotechnology, University of Modena and Reggio Emilia, via Campi 287, Modena 41125, Italy

[3] Department of Life Sciences, University of Modena and Reggio Emilia, via Campi 287, 41125 Modena, Italy

The first event of vision in dim-light conditions is the absorption of a photon by rhodopsin, which causes the *cis-trans* isomerization of 11-*cis*-retinal and a conformational change to its active state (metarhodopsin II, MII state). MII activates heterotrimeric GDP-bound transducin by catalyzing the exchange of GDP for GTP. In that respect, as all GPCRs, MII acts as a guanine nucleotide exchange factor (GEF). Upon dissociation from the βγ dimer, the Gtα-GTP complex stimulates in turn the activation of phosphodiesterase (PDE), thus decreasing the cytoplasmic concentration of cGMP leading to channel closure. Rapid inactivation of MII requires phosphorylation of MII by rhodopsin kinase followed by binding to visual arrestin (arrestin 1 (Arr1)). Deactivation of Gtα requires the hydrolysis of GTP to GDP by the GTPase activity of Gtα, which is catalyzed by a member of the regulators of G protein signaling (RGS) family, acting as a GTPase activating protein (GAP). Complete recovery of the photoresponse requires also restoration of cytoplasmic cGMP to the dark level by the intervention of guanylate cyclase (GC) and calcium-sensing guanylate cyclase-activating proteins (GCAPs) [45, 79].

GPCRs, including rod opsin, undergo dimerization/oligomerization, as an essential component of their life cycle (reviewed in refs [15, 93, 101, 116, 121]).

Another feature of GPCRs is that they can be constitutively active [28, 86], i.e., they can be activated in the absence of an agonist. Constitutively active mutants (CAMs) of GPCRs have been linked to a number of human diseases (reviewed in refs [4, 143, 158, 160]). Diseases can be caused either by activating mutations ("gain-of-function" mutations) or by deactivating mutations ("loss of function" mutations) of GPCRs. Spontaneous mutations in any player of visual phototransduction have been found associated with retinal disease including autosomal congenital stationary night blindness (adCSNB) and autosomal dominant/recessive retinitis pigmentosa (adRP and arRP). While adCSNB is essentially linked to gain-of-function mutations, adRP is mainly linked to loss-of-function mutations. RP comprises a class of hereditary diseases causing the progressive degeneration of the photoreceptor system [54] and visual impairment in 1.5 million patients worldwide [40]. RP affects about 1 in 3000–7000 people, being the most common cause of inherited blindness in developed countries [40, 73, 100]. Predominantly affected are rod cells that aggregate and progressively affect cone cell viability [125]. More than 40 genes have been linked to this hereditary disease. Mutations of the *RHO* gene represent the most common cause of RP, accounting for 25% of adRP and 8 to 10% of all RP. The majority of the over 140 missense mutations found in *RHO* are linked to adRP [18].

adRP *RHO* mutants have been subjected to extensive biochemical and cellular characterizations, leading to a classification into three major groups (I, IIa/II, and IIb/III) (reviewed in [18, 82]), based on rod opsin ability to reconstitute with 11-*cis*-retinal and to be retained into endoplasmic reticulum (ER) [82]. In detail, class I mutants resemble wild type (WT) in ability to regenerate with 11-*cis*-retinal and subcellular localization. In contrast, class IIa (or II in [82]) and class IIb (or III in [82]) mutants show altered membrane localization in their opsin state associated with ability or inability, respectively, to regenerate with 11-*cis*-retinal in vitro.

Another classification of *RHO* mutants linked to adRP and adCSNB is based on a number of variegate effects on rod opsin function (classes 1–7) [5, 100]. The considered effects that found this alternative classification include post-Golgi trafficking and outer segment targeting (class 1), ER retention and impairment in 11-*cis*-retinal binding (class 2), vesicular trafficking and endocytosis (class 3), post-translational modifications (class 4), Gt activation (class 5), constitutive activation (class 6), and efficiency to dimerize (class 7) [5, 100].

The majority of the over 140 *RHO* mutants linked to adRP are likely misfolded and variedly retained into ER (reviewed in [5, 18, 82, 127]). Proteins are monitored by a quality-control system (QCS) in the ER that can retain misfolded structures in the ER for their subsequent degradation (reviewed in [27]). QCS is able to recognize general "errors," e.g., non-native solvent exposure of hydrophobic regions, defects in secondary structures and their packing interactions, unpaired cysteines, or immature glycans (reviewed in [27]), thus preventing protein aggregation. The etiology of conformational diseases can be due to proteins that are either misfolded immediately after synthesis or undergo post-translational conformational alterations. Intracellular GPCR oligomerization can lead to either cell-surface targeting or misrouting. Misrouted mutant GPCRs, when co-expressed with the WT form, can cause intracellular retention of the WT receptor via oligomerization, thus exerting a dominant-negative effect (reviewed in [27]). ER retention by misfolded rod opsin mutants causes ER stress [91], to which cells respond by activating a signaling network called the unfolded protein response (UPR). As a conformational disease [27, 90, 137], adRP linked to *RHO* mutations is amenable to treatment with pharmacological chaperones, small molecules that bind specific sites within a protein native or quasi-native structure, thereby shifting the folding equilibrium towards the native state, thus allowing correct routing. adRP *RHO* mutants that respond to small chaperones like 11-*cis*-retinal can be seen as structurally less stable than the native state due to the loss of some native intramolecular interactions, which is recovered by the small chaperone. Pharmacological therapies for misfolding diseases are based on either promoting correct folding, inhibiting aggregation, increasing degradation, or protecting from cell death [99, 100]. Thus, pharmacological chaperones for misfolded mutant opsins have to intervene early in protein synthesis and folding to compensate for the observed decrease in opsin stability leading to rod and cone cell death [99].

This review article focuses on the advances into rod opsin structure and their implication in our understanding of the determinants of adCSNB and adRP.

Structural models of the dark state of vertebrate rhodopsin

Rod opsin is the founder of family A GPCRs and the best source of high-resolution information on the homologous receptors.

The first highly resolved structure of bovine rhodopsin, deposited in the protein data bank (PDB, http://www.wwpdb.org/) under the identifier 1F88, showed all major structural features, which had been predicted by years of biochemical, biophysical, and bioinformatics studies [118].

Bovine rod opsin contains 348 amino acids, which fold into seven TM helices, varying in length from 19 to 34 residues, and one cytoplasmic helix, H8. All the seven TM helices, except for H3, hold a number of irregularities, e.g., kinks, twists, and bends (Fig. 1a), due to the presence of glycines, prolines, or threonines. Such irregularities are also present in all rod opsin structures successively released. All helices, except for H4 and H7, are tilted from the membrane normal [118].

Rhodopsin family GPCRs share a few highly conserved amino acids distributed in all TM helices. They include N55(1.50), N78(2.45), D83(2.50), C110(3.25), E134(3.49), R135(3.50), Y136(3.51), W161(4.50), P215(5.50), Y223(5.58), F261(6.44), W265(6.48), P267(6.50), N302(7.49), P303(7.50), and Y306(7.53) (the numbering in parentheses follows the arbitrary scheme by Ballesteros and Weinstein [8]; the first number identifies the helix number, whereas the two numbers after the dot indicate the position relative to a reference residue among the most conserved amino acids in the helix; such a reference residue is arbitrarily assigned the number 50). The cytosolic extension of H3 holds the highly conserved E/DRY motif. In the inactive state of rhodopsin (i.e., in the dark), R135(3.50), which in rod opsin is an adRP mutation site, forms a double salt bridge with both the adjacent glutamate, E134(3.49) and E247(6.30) (Fig. 1b) [118]. Both the E3.49-R3.50 and R3.50-E6.30 interactions would contribute to maintain the inactive state of rhodopsin family GPCRs, based on the results of in vitro and computational experiments (reviewed in [35]). The higher degree of conservation of D/E3.49 than E6.30 would, however, make the former residue more relevant than the latter in stabilizing the resting state. Together with H3, H6 is the second longest helix. Its cytosolic half is almost perpendicular to the membrane plane, whereas its extracellular half is bent, because of

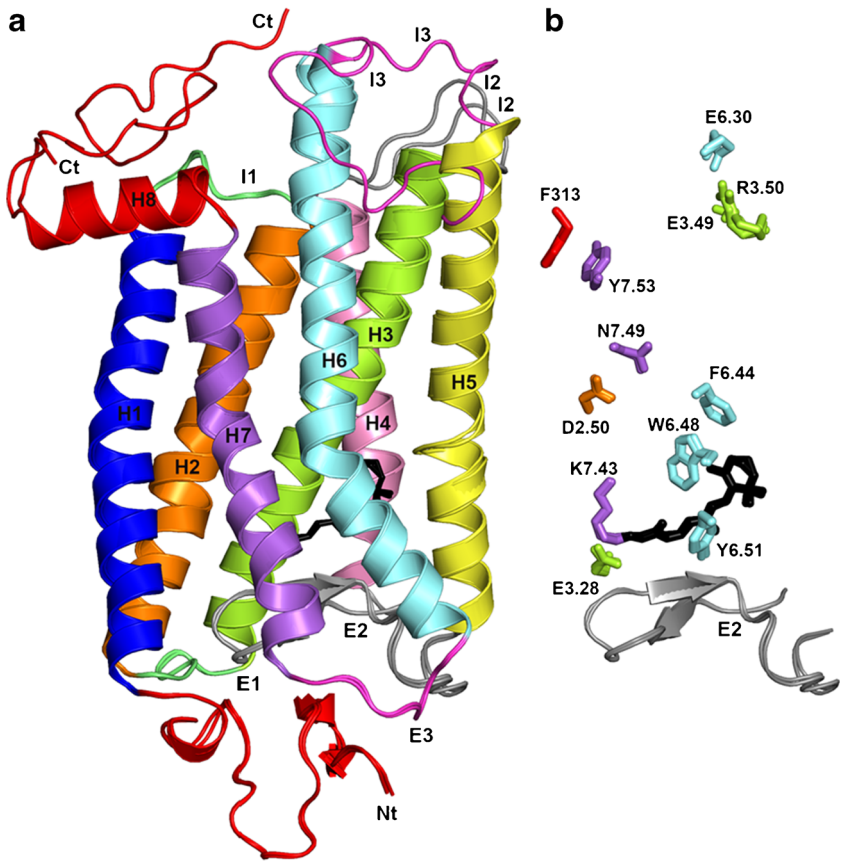

Fig. 1 Side view, in a direction parallel to the membrane surface, of the superimposed highest resolution dark rhodopsin structures (PDB: 1U19 [113] and 1GZM [87]). On the left side, a cartoon representation of the whole structures is shown, including the 11-*cis*-retinal, represented by black sticks. On the right side, a stick representation of selected highly conserved amino acids in the seven-helix bundle is shown. The cytosolic side is at the top. H1, H2, H3, H4, H5, H6, and H7 are, respectively, colored in blue, orange, green, pink, yellow, cyan, and violet; Nt and Ct, the latter including H8, are red, I1 and E1 are lime, I2 and E2 are gray, and I3 and E3 are magenta

P267(6.50), which in rod opsin is an adRP mutation site (Fig. 1a) [6, 7, 102]. H6 holds the conserved FxxCWxPY motif forming an aromatic cluster, with W265(6.48) and Y268(6.51) participating in 11-*cis*-retinal binding. H7 contains a 3.10 helical stretch in the region around the retinal attachment site, K296(7.43), and two prolines, P291(7.38) and P303(7.50), the latter belonging to the highly conserved NPxxY motif. The tyrosine of this motif is involved in π-π stacking interactions with F313 in H8 (Fig. 1b).

Packing of the cytosolic regions diverges from that of the intradiscal regions, the latter being significantly associated with each other and well resolved, contrarily to the former. Indeed, the Nt holds a β-hairpin forming a four-stranded antiparallel β-sheet with the β-hairpin in E2 that plugs the retinal, which has to enter through pores opened in between the TM helices [139]. E2 is engaged in a disulfide bridge with C110(3.25). Both C110(3.25) and C187 are sites of adRP misfolding mutations, indicating the relevance of the bridge in rhodopsin stability.

The most resolved rhodopsin structure, 1U19, holds the complete backbone [112, 113, 118, 159]. Li et al. resolved a rhodopsin structure at 2.65 Å (PDB: 1GZM) [87] by molecular replacement from the 1F88 structural model [118]. Like 1U19, 1GZM also resolves all the interhelical loops. The most significant main chain differences between 1GZM and 1U19 reside in I2, I3, and the C-terminal segment following H8 (Fig. 1a), the latter being disordered in 1GZM [87, 113]. Other differences between 1U19 and 1GZM concern the retinal ring, whose conformation in 1GZM is the same as in 1F88 [87, 113, 118] (Fig. 1a).

Insights into vertebrate rod opsin photobleaching from spectroscopic and structure determinations

Vertebrate rod opsin is the GPCR best characterized at atomic resolution in its inactive and active states. To date, a number of crystal structures of bovine rhodopsin have been released, which correspond to different states in the photoactivation cascade (Table 1). These include (a) rhodopsin in the dark state [87, 94, 112, 113, 118, 135, 150, 159]; (b) rhodopsin containing the non-native chromophore 9-*cis*-retinylidene (isorhodopsin) [104], or a 6-carbon-ring retinal [53], or octyl beta-D-glucopyranoside; (c) two early photointermediates [105, 106]; (d) a thermostabilized mutant in the dark state [149]; (e) a photoactivated deprotonated intermediate [135]; (f) the active opsin (Ops*) apoprotein both in its free state [120] and in complex with the Ct of transducin (GtCt) [13, 141]; (g) Ops* in complex with non-retinoid ligands [13, 95, 119]; (h) the E113Q CAM bound to all-*trans*-retinal and the GtCt peptide [148]; (i) MII both in its free and GtCt-bound forms [24]; (j) G90D and T94I CSNB mutants [146, 147]; (k) the cryoEM structure of an inactive opsin dimer [169]; (l) rhodopsin in complex with G proteins [46, 63, 68, 161, 162]; (m) dimeric opsin in complex with the finger loop of Arr1 [156]; and (n) opsin bound to Arr1 [67, 170, 171] (Table 1).

Photochemical experiments allowed definition of the reaction coordinates of rhodopsin activation [97, 111]. Photoactivation of rod opsin include (1) *cis-trans* isomerization of the retinal, (2) thermal relaxation of rhodopsin complex, and (3) formation of the signaling active states (reviewed in refs [59, 97, 111]).

Photobleaching of rhodopsin involves different intermediates (Fig. 2) [9, 55, 77, 111, 167].

Following photon absorption and electronic excitation, fast isomerization of the chromophore leads to formation of bathorhodopsin (BATHO, 529 nm) (Fig. 2) on the fs time scale (i.e., in 200 fs). BATHO is in equilibrium with the blue-shifted intermediate (BSI, 477 nm), which decays to lumirhodopsin (LUMI, 492 nm) in 150 ns. Whereas the BATHO to BSI transition involves conformational changes of retinal, the BATHO to LUMI transition is accompanied by a movement of the β-ionone ring away from W265(6.48) (Fig. 2). Indeed, the distorted all-*trans* retinal in the BATHO structure (PDB: 2G87) dislocates its β-ionone ring in the LUMI intermediate (PDB: 2HPY) [105, 106]. The adRP mutation site, E181 (in E2), would be charged in the BATHO state [136]. LUMI transforms to metarhodopsin I (MI, 478 nm) in 10 μs. MI formation would not involve large helix movements, but only a rearrangement close to the bend of H6, at the level of the retinal chromophore [133]. These results indicate that rhodopsin remains in a ground state-like conformation until late in the photobleaching process, the gross conformational changes occurring in the MI to MII transition, the only one occurring on a slow time scale (i.e., 1 ms) [133]. The transition depends on and probably involves protonation of E134(3.49), which would require the presence of transducin [3, 34, 111]. Protonation of E134(3.49) of the E/DRY motif would destabilize the salt bridge between E134(3.49) and R135(3.50), releasing an important constraint of the inactive state. This hypothesis is supported by the findings that the E134Q mutation induces constitutive activation of rod opsin [26]. Proton translocations to E134(3.49) and E113(3.28) can be decoupled, corresponding to the MII_a and MII_b states (Fig. 2) [3, 111]. According to this model, the transition of MI to MII_a is accompanied by translocation of the SB proton to E113(3.28), whereas MII_b formation requires also proton uptake from the cytoplasm, with a pH-dependent ΔG [111]. Formation of the signaling active state would merely be a release of constraints in the helix bundle, leading to the exposure of cytosolic portions deputed to G protein recognition. Spectroscopic studies on rhodopsin allowed an extension of the MI↔MII_a↔MII_b to MI↔MII_a↔MII_b↔MII_bH^+ equilibrium scheme, meaning that H6 motions accompanying MII_b

Table 1 X-ray structures of vertebrate rod opsins

Accession ID	Resolution (Å)	Release date	Molecular system	Ref.
1F88	2.80	2000-08-04	Bovine rhodopsin with 11-*cis*-retinal	[118]
1HZX	2.80	2001-07-04	Bovine rhodopsin with 11-*cis*-retinal	[159]
1L9H	2.60	2002-05-15	Bovine rhodopsin with 11-*cis*-retinal	[112]
1GZM	2.65	2003-11-20	Bovine rhodopsin with 11-*cis*-retinal	[87]
1U19	2.20	2004-10-12	Bovine rhodopsin with 11-*cis*-retinal	[113]
2HPY	2.80	2006-08-22	Bovine lumirhodopsin with all-*trans*-retinal	[106]
2G87	2.60	2006-09-02	Bovine bathorhodopsin with all-*trans*-retinal	[105]
2I35	3.80	2006-10-17	Bovine rhodopsin with 11-*cis*-retinal	[135]
2I36	4.10	2006-10-17	Bovine rhodopsin with 11-*cis*-retinal[a]	[135]
2I37	4.15	2006-10-17	Bovine rhodopsin with all-*trans*-retinal[a]	[135]
2J4Y	3.40	2007-09-25	Mutant bovine rhodopsin with 11-*cis*-retinal	[149]
2PED	2.95	2007-10-30	Bovine rhodopsin with 9-*cis*-retinal	[107]
3CAP	2.90	2008-06-24	Bovine opsin (dimer)	[120]
3C9L	2.65	2008-08-05	Bovine rhodopsin with 11-*cis*-retinal	[150]
3C9M	3.40	2008-08-05	Bovine rhodopsin with 11-*cis*-retinal	[150]
3DQB	3.20	2008-09-23	Bovine opsin in complex with GtCt	[141]
3OAX	2.60	2011-01-19	Rhodopsin with beta ionone	[94]
3PQR	2.85	2011-03-09	Bovine rhodopsin with all-*trans*-retinal and GtCt	[24]
3PXO	3.00	2011-03-09	Bovine rhodopsin with all-*trans*-retinal	[24]
2X72	3.00	2011-03-16	Bovine rhodopsin CAM with GtCt	[148]
4A4M	3.30	2012-01-25	N2C, M257Y,D282C bovine rhodopsin CAM with GtCt	[31]
4BEZ	3.20	2013-04-24	G90D CSNB bovine opsin mutant	[147]
4BEY	2.90	2013-05-08	G90D CSNB bovine opsin mutant with GtCt	[147]
4J4Q	2.65	2013-10-30	Bovine opsin with octylglucoside	[119]
4PXF	2.75	2014-09-17	Bovine opsin with the finger loop of visual arrestin	[156]
4X1H	2.29	2015-11-04	Bovine opsin with nonyl-glucoside and GtCt	[13]
4ZWJ	3.30	2015-07-29	Human opsin bound to visual arrestin	[67]
5DGY	7.7	2016-03-23	Human rhodopsin bound to visual arrestin	[170]
5DYS	2.3	2016-08-10	T94I CSNB bovine rhodopsin CAM	[146]
5EN0	2.81	2016-08-10	T94I CSNB bovine rhodopsin CAM with GtCt	[146]
5TE3	2.7	2017-03-15	Bovine opsin	[53]
5TE5	4.01	2017-03-15	Bovine rhodopsin with 6-carbon ring retinal	[53]
5W0P	3.01	2017-08-09	Human opsin bound to visual arrestin	[171]
6FKA,B,C,D ,6,7,8,9	2.7	2018-04-04	Bovine opsin with stabilizing ligands	[95]
6CMO	4.5	2018-06-20	Human opsin bound to heterotrimeric Gi	[68]
6FUF	3.12	2018-10-03	Bovine rhodopsin with all-*trans*-retinal and mini Go	[162]
6OYA	3.30	2019-07-24	Bovine rhodopsin with all-*trans*-retinal, and heterotrimeric mini Gt	[46]
6OY9	3.9	2019-07-24	Bovine rhodopsin with all-*trans*-retinal and heterotrimeric mini Gt	[46]
6QNO	4.38	2019-07-10	Bovine rhodopsin with all-*trans*-retinal and heterotrimeric mini Gi	[161]
6OFJ	4.5	2019-08-21	Bovine opsin dimer (inactive)	[169]

formation lead to the MII_bH^+ state following proton uptake by E134(3.49) from the cytosol (Fig. 2) [78]. The latter would be important for GDP release from Gt [138].

Initial deactivation of MII relies on opsin interaction with its kinase, which phosphorylates the receptor promoting tight binding to Arr1 [114, 124]. Full deactivation requires

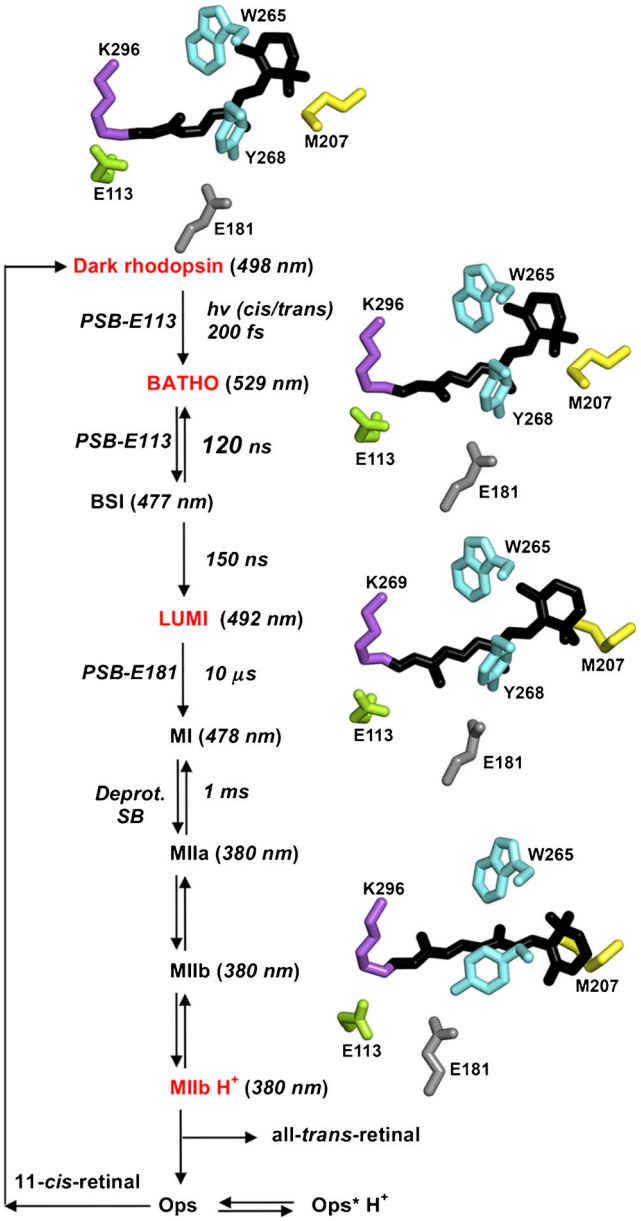

Fig. 2 Rhodopsin photobleaching. The process of rhodopsin photoactivation is schematized here. The retinal and selected surrounding amino acid residues are represented as sticks for the dark, BATHO, LUMI, and MIIb H+ states (highlighted in red)

rhodopsin regeneration [38, 56]. This requires the hydrolysis of the all-*trans* SB and depletion of all-*trans*-retinal from the active site, a step that requires the nucleophilic attack of structural water in the hydrophobic retinal binding site [38, 56]. Formation of opsin is accompanied by increase in intrinsic tryptophan fluorescence after releasing all-*trans*-retinal from the active site [38, 56]. The retinal remains associated with opsin membranes and is converted by endogenous NADPH-dependent retinol dehydrogenase (RDH, reviewed in ref [97]) to all-*trans*-retinol. During the MII decay, a storage form of rhodopsin, metarhodopsin III (MIII), is generated. The formation of MIII can be induced by blue light absorption in MII, passing through the anti-syn isomerization form or "reverted-Meta" intermediate MIII, and the subsequent reprotonation of the Schiff base [55, 132]. It has been inferred that, in addition to the retinylidene pocket (site I), there are other two retinoid-binding sites within opsin: site II, the entrance site, and site III, the exit site. The latter is occupied when retinal remains bound after its release from site I [139]. The MIII form is suggested to hold photolyzed all-*trans*-retinal bound in site III. Opsin finally returns to the ground state via a transiently formed opsin-11-*cis*-retinal complex, which contains both retinal isomers bound to site II and site III [139].

The activity of ligand-free opsin is 10^6 times lower than the activity of the all-*trans*-retinal-bound active MII state, but it is higher than the activity of dark rhodopsin, thus indicating that 11-*cis*-retinal acts as an inverse agonist [98, 111]. Lower pH enhances opsin activity likely due to protonation of E134(3.49) [59, 141].

X-ray determination of bovine Ops* structure (PDB: 3CAP [120]) provided a significant advancement in our understanding of ligand-independent GPCR activation. SB hydrolysis makes MII unstable and difficult to crystallize. The crystal structure of the MII state was, therefore, obtained by soaking the Ops* crystals with all-*trans*-retinal forming a SB with K296(7.43) [24]. Such structure, released both in its free state (PDB: 3PXO [24]) and in complex with the GtCt peptide (PDB: 3PQR [24]), as well as the structure of the E113Q CAM in complex with GtCt (PDB: 2X72 [148]), are almost identical to the corresponding free and GtCt-bound states of Ops*.

Major structural differences between dark rhodopsin and Ops*/MII essentially concern the cytosolic halves of H5, H6, H7, and I3 (Fig. 3). Indeed, H5 is longer in Ops*/MII than in dark rhodopsin, with its cytoplasmic end shifted by 2–3 Å towards H6. The cytosolic end of H6 is tilted from H3 by 6–7 Å (Fig. 3c). These displacements are associated with the breakage of both the salt bridge interactions involving R135(3.50) in the resting dark state. This is accompanied by the establishment of novel interactions between, (a) R135(3.50) and the conserved Y223(5.58) and (b) E247(6.30) and K231(5.66). Moreover, the conserved Y306(7.53) of the NPxxY motif rotates to face the helix bundle, thereby blocking H6 from moving back towards H3 in an inactive state conformation (Fig. 3b).

The opening of a cytosolic crevice in between H3 and H6, which follows the outward movement of H6, is instrumental in forming the docking site for transducin, as shown by the crystallographic complexes between Ops*/MII/E113Q and GtCt (PDB: 3DQB [141], 3PQR [24], and 2X72 [148], respectively).

The striking similarity between Ops* and MII structures contrasts with differences in their coupling efficiency to transducin.

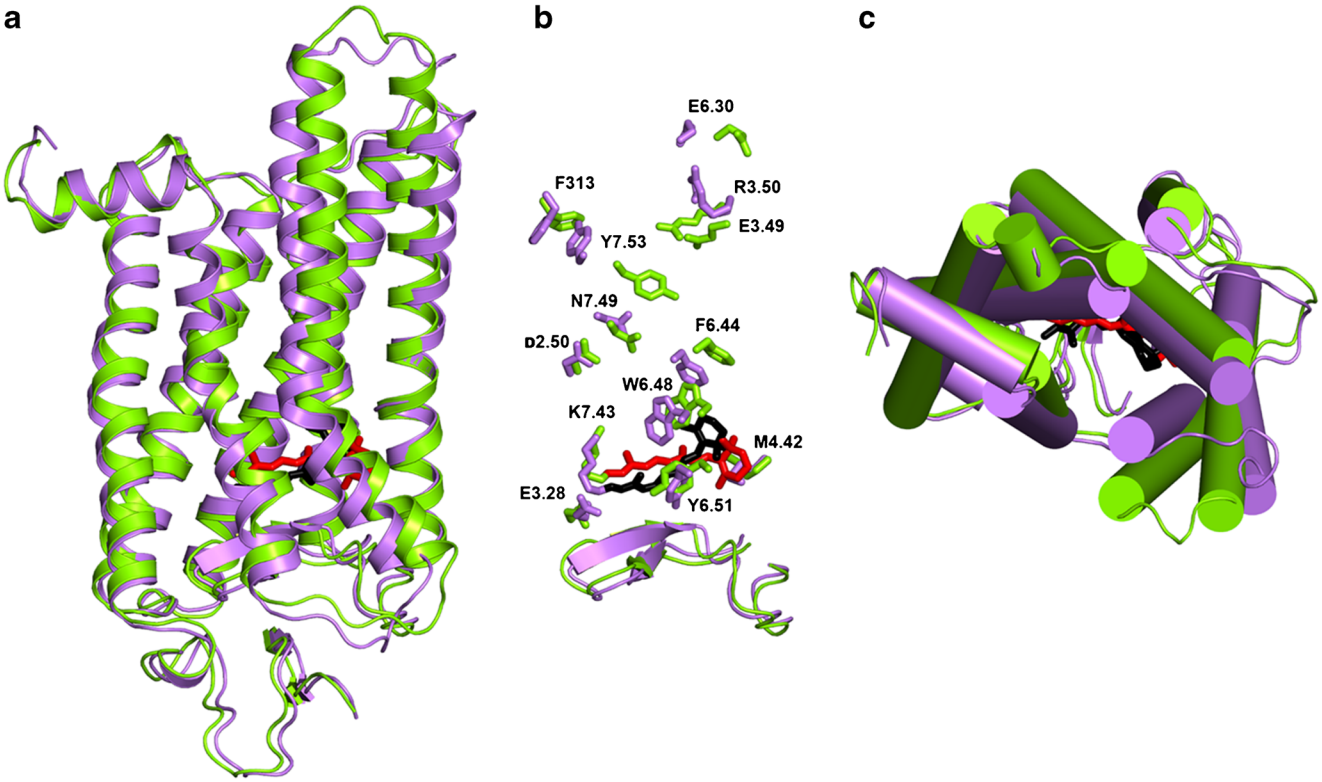

Fig. 3 Structural comparisons of active and inactive rod opsin structures. Cartoons of the superimposed structures of dark rhodopsin (PDB: 1GZM, violet [87]) and MII (PDB: 3PXO, green [24]) are shown. The helix bundles are seen both in a direction parallel to the membrane surface with the cytosolic side being at the top (**a** and **b**) and from the cytosolic side in a direction perpendicular to the membrane surface (**c**). The side chains of selected highly conserved and of retinal binding site amino acids and the backbone of E2 are shown (**c**). The 11-*cis*-retinal and all-*trans*-retinal are represented as black and red sticks, respectively

The structures of activated opsin in complex with stabilizing detergents or other small compounds bound onto or near the orthosteric retinal binding site provide valuable targets for structure-based discovery/design of stabilizing non-retinoid ligands [13, 95, 119].

Structures of signaling active rod opsin states in complex with G proteins or visual arrestin

Since very recently, the structures of rod opsin in ternary (i.e., with bound all-*trans*-retinal) or binary (in the apo state) complexes with heterotrimeric Go, Gi, or Gt have been released providing insights into a fundamental step in visual phototransduction [46, 63, 68, 162].

Heterotrimeric G proteins belong to the α-family of the Ras GTPase superfamily. Gα proteins are made of two domains, the Ras-like or GTPase (G) domain, which is shared by all Ras GTPases, being deputed to GDP/GTP binding and GTP hydrolysis, and a helical (H) domain [165].

The following structural description of the α-subunit employs the Noel's nomenclature (Fig. 4a, b) [108].

The G domain holds a Rossmann fold, characterized by a 3-layer(αβα) sandwich architecture holding a five-stranded parallel β-sheet sandwiched between two layers of α-helices, α1 and α5, on one side, and α2, α3, and α4 on the other side. The β1/α1, α1/β2 (αF/β2 in the Gα proteins), β3/α2, β5/α4, and β6/α5 loops (i.e., G boxes 1-5 (G1-G5)) hold sequence conservation and are deputed to nucleotide binding (Fig. 4). G1, the β1/α1 loop, is also named P-loop (phosphate-binding loop) as it contacts the phosphates through main-chain NH groups and lysine side chain. G2, the α1/β2 loop (αF/β2 loop in the Gα proteins), is also called switch I (swI). G3 is part of the switch II (swII), which is made of the β3/α2 loop plus the α2-helix. G4 and G5 are, respectively, the β5/α4 and β6/α5 loops, which make contacts with the guanine base.

Differently from small Ras GTPases, Gα proteins hold a third switch, swIII, that is the loop connecting β4 to α3 [108] as well as the H domain made of six helices (αA-αF) organized in an orthogonal bundle architecture and a Gi alpha 1, domain 2-like topology. The loops that connect G and H domains are linker1 (the α1/αA loop) and linker 2 (the αF-β2 loop corresponding to the swI) (Fig. 4). The nucleotide, GDP or GTP, binds at the interface between G and H domains (Fig. 4a).

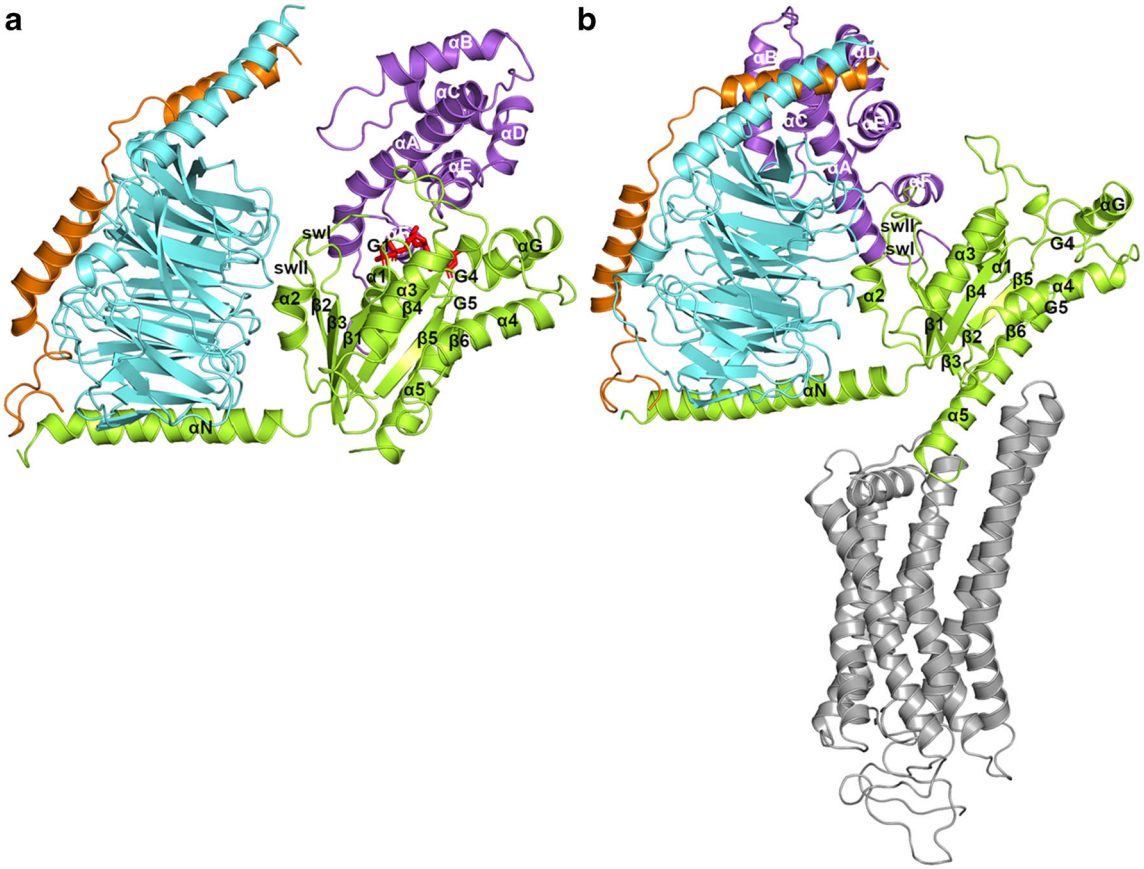

Fig. 4 OFF and GEF-bound states of heterotrimeric Gi. The inactive GDP-bound state (**a**) and the nucleotide-free opsin-bound states (**b**) of heterotrimeric Gi are shown. The G and H domains of the α-subunit are green and violet, respectively, the β- and γ-subunits are aquamarine and orange, respectively, and opsin is gray. In the inactive-state structure (**a**), the GDP bound in between the G and H domains of the α-subunit is represented as red sticks. In all panels, the secondary structure elements are labeled according to Noel's nomenclature [108]

In heterotrimeric G proteins, the β-subunit holds a 7-propellor architecture and a methylamine dehydrogenase topology, whereas the γ-subunit holds an irregular architecture of two α-helices connected by a loop and a G Protein Gi Gamma 2 topology.

The signaling active states of GPCRs, in general, and of rod opsin, in particular, recognize the Ct of α5 and the α/β loops of the Gα G domain, which are distal from the nucleotide binding site [129]. The first insights into the mechanism of GPCR-catalyzed GDP release arose from molecular simulations and biophysical determinations as well as from structure determination of the ternary complex made of agonist-bound β2-adrenergic receptor (β2AR) and nucleotide-free heterotrimeric Gs [41, 49, 74, 126, 129, 140, 153, 163]. These experiments indicated that, by acting on the orientation of α5 and on the conformation of G5, GPCRs weaken the contacts between GDP and G domain accompanied by a detachment of the H domain from the G domain, ultimately leading to GDP release [41, 49, 74, 126, 129, 140, 153, 163].

The structures of rod opsin in complex with heterotrimeric G proteins confirmed the gross binding mode of the G domain to the cytosolic regions of the receptor as found in the β2AR-Gs complex (PDB: 6CMO, 6FUF, 6OYA/B, 6QNO [46, 63, 68, 162]). In particular, α5 of Gα docks in between H3 and H6 and contacts H8 of rod opsin, whereas αN of Gα interacts with I2 of rod opsin (Fig. 4b). Differences, however, occur in the way GsCt and GiCt/GtCt dock onto the cytosolic cleft of β2AR and rod opsin, respectively [46, 63, 68, 129, 162]. Indeed GiCt or GtCt make a more extended hydrophobic interface with H6 of rod opsin than GsCt does with H6 of β2AR. This may be responsible for the different conformational behavior of H6, whose outward motions would be less pronounced for Gi-bound rod opsin than Gs-bound β2AR [46, 63, 68, 129, 162]. This different dynamics, likely linked to chemico-physical differences in the GαCt-H6 interface, might determine receptor-G protein coupling specificity [68].

Three out of the four opsin-G protein complexes released so far concern mini G proteins bearing only the G domain [46, 63, 68, 162]. In the cryoEM structure of rod opsin in complex with heterotrimeric Gi holding both domains, a dominant-negative mutant form of Gi was used to promote the nucleotide-free form of the G protein [68]. Such complex displays a detachment of the H domain from the G domain, though less marked compared to the one seen in the β2AR-Gs

complex [46, 63, 68, 129, 162]. These structural models strengthen the evidence that interdomain motion is an essential step in the process of GDP depletion from Gα.

The cryoEM structure of rod opsin and heterotrimeric mini Gi shows that the receptor Ct interacts with the Gβ subunit of the G protein, providing a structural foundation for the role of Ct in GPCR signaling and of Gβ as a scaffold for recruiting Gα subunits and G protein-receptor kinases [63]. The study suggests that the observed interaction between the central part of opsin Ct (OpsCt) and Gβγ is instrumental in localizing the G protein heterotrimer to the active receptor first. After dissociation of the Gα subunit, a transient Gβγ-receptor complex could provide the adequate molecular framework for receptor phosphorylation by bringing the kinase close to the OpsCt [63].

Providing insights into opsin GEF action and the linked mechanism of G protein activation, structure determinations of opsin-G protein complexes represent invaluable frameworks to infer the determinants of inherited retinal diseases affecting opsin-transducin coupling. In this respect, non-misfolded adRP rod opsin mutants such as M44T and V137M (in positions 1.39 and 3.52, respectively), both located in the cytosolic end of rod opsin helix bundle, have been found to alter opsin-transducin coupling by accelerating the early steps of transducin activation, without increasing the basal activity of the G protein [2]. Moreover, rod opsin mutants linked to CSNB, e.g., G90D, constitutively activate transducin by perturbing the SB [147].

Upon phosphorylation by receptor kinases, rod opsin undergoes fast desensitization by binding to visual arrestin (Arr1). Arr1, which, differently from Arr2 and Arr3, is uniquely deputed to recognize opsins, holds a β-sandwich architecture and an immunoglobulin-like topology made of N-terminal (residues 8-180) and C-terminal (residues 188-362) domains (ND and CD, respectively) (Fig. 5a).

Each domain is made of a seven-stranded β-sandwich plus an additional lateral strand [58]. The sandwich comprises a four-stranded β-sheet packed against a three-stranded β-sheet. ND contains a single α-helix, while CD contains two short 3_{10} helices (Fig. 5a) [58]. The terminal residues of the protein, "C-tail" (residues 372–404), are connected by a flexible linker (residues 362-371) to CD (Fig. 5a). In the resting state, the C-tail forms a parallel β-sheet with the lateral strand of ND. The topology of the two domains is such that three loops, i.e., finger loop (residues 68–78), middle loop (residues 133–142), and C-loop (residues 248–253) form a central crest. The finger loop is a key receptor-binding element (Fig. 5a) [142]. The interface of ND and CD is stabilized by a number of interactions including those in the so-called polar core. Receptor-arrestin recognition would occur in two steps. In the first step, the phosphorylated receptor Ct (OpsCt, in the case of opsin) displaces the C-tail of arrestin and recognizes positively charged amino acids on ND, thus forming a low affinity pre-complex. The second step, triggered by interdomain movements, is characterized by binding of a number of arrestin loops, including finger, middle, and lariat (residues 281–321) loops, to the cytosolic regions of the receptor, thus forming a high-affinity complex [57, 142].

Advances in structure determinations shed light on the mechanisms of arrestin activation. The active-state structures of Arr1 concern a naturally occurring constitutively active form called p44 (PDB: 4J2Q) [75] and the opsin-bound state. The recent structure of phosphorylated opsin in complex with Arr1 (PDB: 5W0P) unveiled the structural characteristics of the high affinity receptor-arrestin complex (Fig. 5c) [171]. The complex is characterized by two interfaces. The primary interface is contributed by interactions between OpsCt and a positively charged crevice in Arr1 ND. The secondary interface concerns the interactions between Arr1 and the receptor core and includes (a) I1, H6, and H8 of opsin and the finger loop of Arr1; (b) I2 of opsin and the middle, lariat, and the 236–265 β-hairpin-strands of Arr1; and (c) H5 of opsin and the C-loop of Arr1 (Fig. 5c). In the opsin-bound state, the finger loop of Arr1 acquires two-turns of α-helix compared to the receptor-free form (Fig. 5b). Other hallmarks of Arr1 activation, inferred from the structural model of opsin-Arr1 complex, include breakage of the polar core, ~21° interdomain rotation about an intramolecular pseudo two-fold axis, and conformational changes within the central crest loops.

Remarkably, Arr1 competes for the same binding site of the G protein, by docking into the cytosolic crevice formed by the outward motion of H6, as an effect of receptor activation (Figs. 4b and 5c). In this respect, structure determinations suggest mutually exclusive binding of G protein and Arr1 to activated opsin. Similarly to the opsin-G protein complexes, the structure of opsin in complex with Arr1 may help inferring the determinants of adRP linked to mutations that affect opsin desensitization and endocytosis. These include mutants at R135(3.50) of the highly conserved E/DRY motif, which is involved both in transducin and Arr1 recognition. The adRP rod opsin mutant R135W was found to be hyperphosphorylated and bound with high affinity to Arr1 in the absence of chromophore, being constitutively internalized [25]. This causes accumulation into rod inner segment and prevents traffic to the outer segment contributing to disease. The presence of a tryptophan in place of R135 would favor the formation of a hydrophobic crevice in opsin that would tightly bind the hydrophobic face (i.e., contributed by I73, M76, and L78) of the finger-loop helix of Arr1, thus explaining in part the high affinity of mutant opsin for Arr1. Remarkably, the adRP-linked mutation of R135 into another hydrophobic amino acid like leucine displays the same phenotype as R135W [1, 25].

Supramolecular organization of rod opsin

The oligomeric state in native membranes was demonstrated years ago for rhodopsin [42, 43]. According to AFM

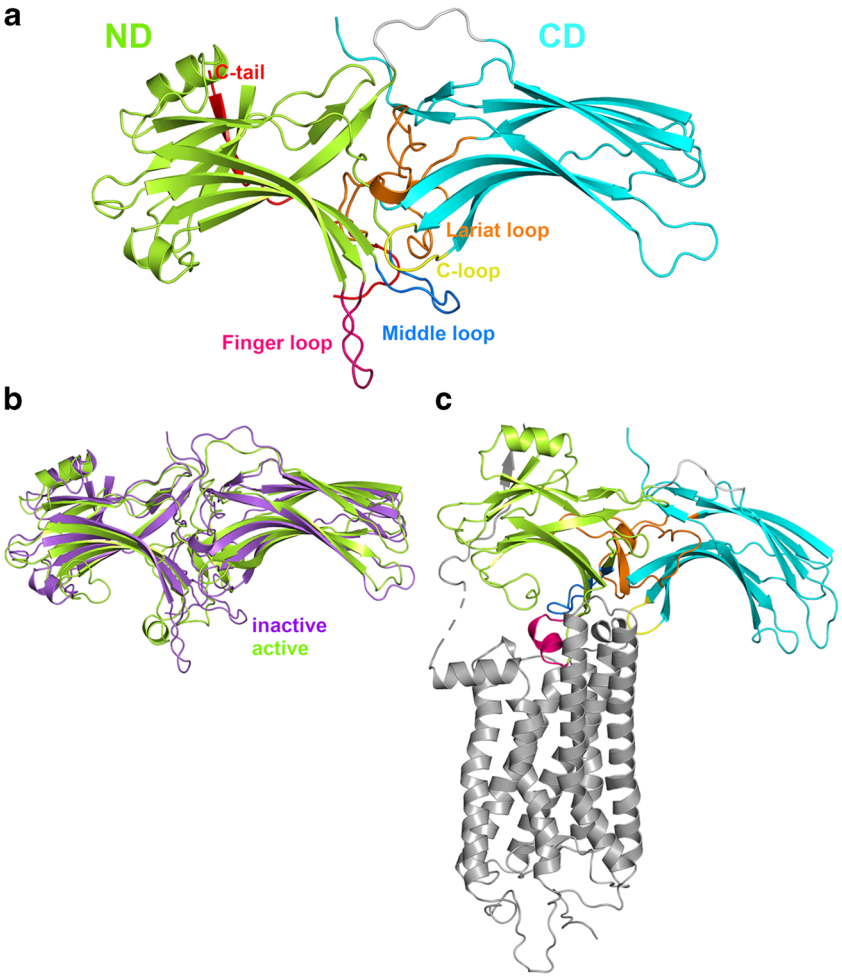

Fig. 5 Visual arrestin structures in the free state and in complex with rod opsin. **a** The inactive state of Arr1 is shown (PDB: 1CF1 [58]). The finger, middle, lariat, and C loops are, respectively, magenta, blue, orange, and yellow. The Ct-tail is red, and the ND and CD are, respectively, green and aquamarine. **b** The superimposed structures of Arr1 in the inactive (violet, PDB: 1CF1 [58]) and opsin-activated (green, PDB: 5W0P [171]) states are shown. **c** The complex between opsin-activated Arr1 (colored as in **a**) and opsin (gray) (PDB: 5W0P [171]) is shown

experiments, the native arrangement of rhodopsin in mouse disk membranes would consist in paracrystalline rows of dimers [43]. The authors also demonstrated that rhodopsin dimers hasten the process of transducin activation by accelerating rhodopsin-transducin recognition [44, 64, 65, 152]. Concentration-dependent oligomerization was also observed by Förster energy transfer (FRET) spectroscopy in Chinese hamster ovary (CHO) cells [52, 103]. Whether rhodopsin oligomerization is an artifact or a physiologic condition has long been debated [19–21, 29, 121].

AFM determinations permitted the building of a semiempirical structural model of oligomeric rhodopsin (PDB: 1N3M, Fig. 6a) [89], made of repeats of the same monomeric unit (i.e., a completed 1HZX structure [159]). According to this model, two monomers of rhodopsin make contacts mediated, for both monomers, by E2, I2, H4, and H5 (Fig. 6a). Contacts between dimers involve I3 and both I1 and Ct (Fig.5a). This oligomeric model was supported by cysteine cross-linking experiments indicating that rhodopsin dimers would rely on W175-W175 (in E2) and Y206(5.41)-Y206(5.41) contacts [81].

Successively, the crystal structure of Ops* (PDB: 3CAP [120]) revealed a divergent dimeric architecture characterized by H1-H1 and H8-H8 contacts, all compatible with AFM images [92]. Consistently, the recent cryoEM structures of a cross-linked rhodopsin dimer and of a rhodopsin dimer reconstituted into nanodiscs from purified monomers show a dimer interface mediated by H1-H1 and H8-H8 contacts (PDB: 6OFJ [169]). An oligomer was also inferred, made of rows of dimers held together by E2-I3 and H4-H6,H5 contacts (Fig. 6b). The authors proposed that the dimer interface and the arrangement of two protomers are necessary for the formation of the rows of dimers [169].

The more recent oligomeric model is consistent with the experimental evidence that the adRP rod opsin mutant F45L in H1 (position 1.40) is impaired in dimerization [123]. Indeed, in the cryoEM opsin oligomer, native F45 contributes to the H1-H1 contacts funding the dimer interface.

Although the role of rod opsin oligomerization awaits clarification, functional characterization of rhodopsin monomers and dimers in detergents demonstrated that monomeric rhodopsin is able to activate transducin, though the oligomeric

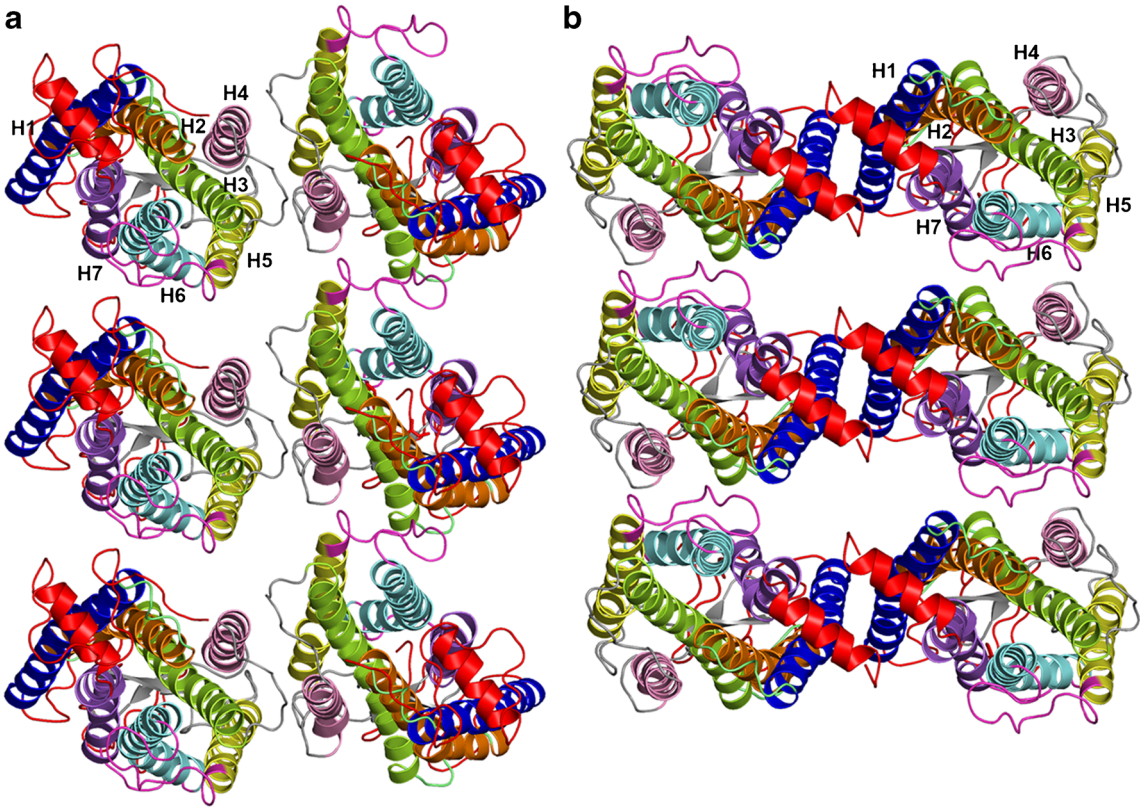

Fig. 6 Structural models of rhodopsin oligomers. Rhodopsin hexamers are shown, which have been obtained by fitting the 1U19 structure onto each monomer onto the 1N3M oligomer [89] (**a**) and onto the oligomeric model inferred from cryoEM (kindly provided by K. Palczewski) (**b**) [169]

form is more active [64, 65]. In vitro experiments in solution and in nanodiscs containing one and two rhodopsin molecules strengthened the evidence that the receptor monomer holds the structural determinants for transducin activation and, in this regard, it is the functional unit [10, 20, 21, 33].

Oligomerization may be essential for the ontogeny and/or desensitization of rod opsin and, hence, in the control of light signaling. Aggregation between WT rod opsin and some partially misfolded adRP *RHO* mutants may have implications in the etiology of the disease and on responsiveness to retinoid chaperones [50, 51]. Addressing these aspects may have important implications in unraveling the molecular determinants of retinal degenerative diseases.

Insights into retinal diseases from structure determinations and computational experiments

Rod cells of human CSNB patients [96, 145] and of animal models carrying the G90D mutation are functionally desensitized, as if they were under constant low basal stimulation that perturbs dim-light vision [32, 66, 144]. The determinants of CSNB linked to CAM opsin would concern (1) constitutive activation of transducin by G90D opsin [66, 128], (2) constitutive activation of opsin caused by thermal isomerization of retinal [145], and (3) constant basal activation by a pre-activated dark state [32].

The crystal structures of G90D (PDB: 4BEY and 4BEZ [147]) and T94I (PDB: 5DYS and 5EN0 [146]) CSNB *RHO* mutants, in their unliganded and all-*trans*-retinal-bound states, provided insights into the structural determinants of the disease. The structural models of the mutants are identical to those of WT apo and all-*trans*-retinal-bound opsin (Fig. 7 a–d). The structure of G90D is characterized by a salt bridge between D90(2.57) and K296(7.43), displacing the retinal counterion E113(3.28) (Fig. 7c). The D90-K296 salt bridge would both stabilize the active state and reduce binding of opsin to the desensitizing Arr1 [147]. Moreover, the interference of G90D with the site of retinal attachment would also increase the rate of thermal isomerization [147]. Several retinal isomers, including all-*trans*- and 11-*cis*-retinal, can transiently activate opsin until protein deactivation by SB formation [72, 80]. Perturbation of SB by CSNB mutations can lead to constitutive activation in the presence of non-covalently bound *cis*-retinal [147].

In T94I rod opsin mutant, the replacing I94 establishes direct van der Waals interactions with K296(7.43), thus prolonging the lifetime of the MII signaling active state [146]. Collectively, a common feature of G90D and T94I

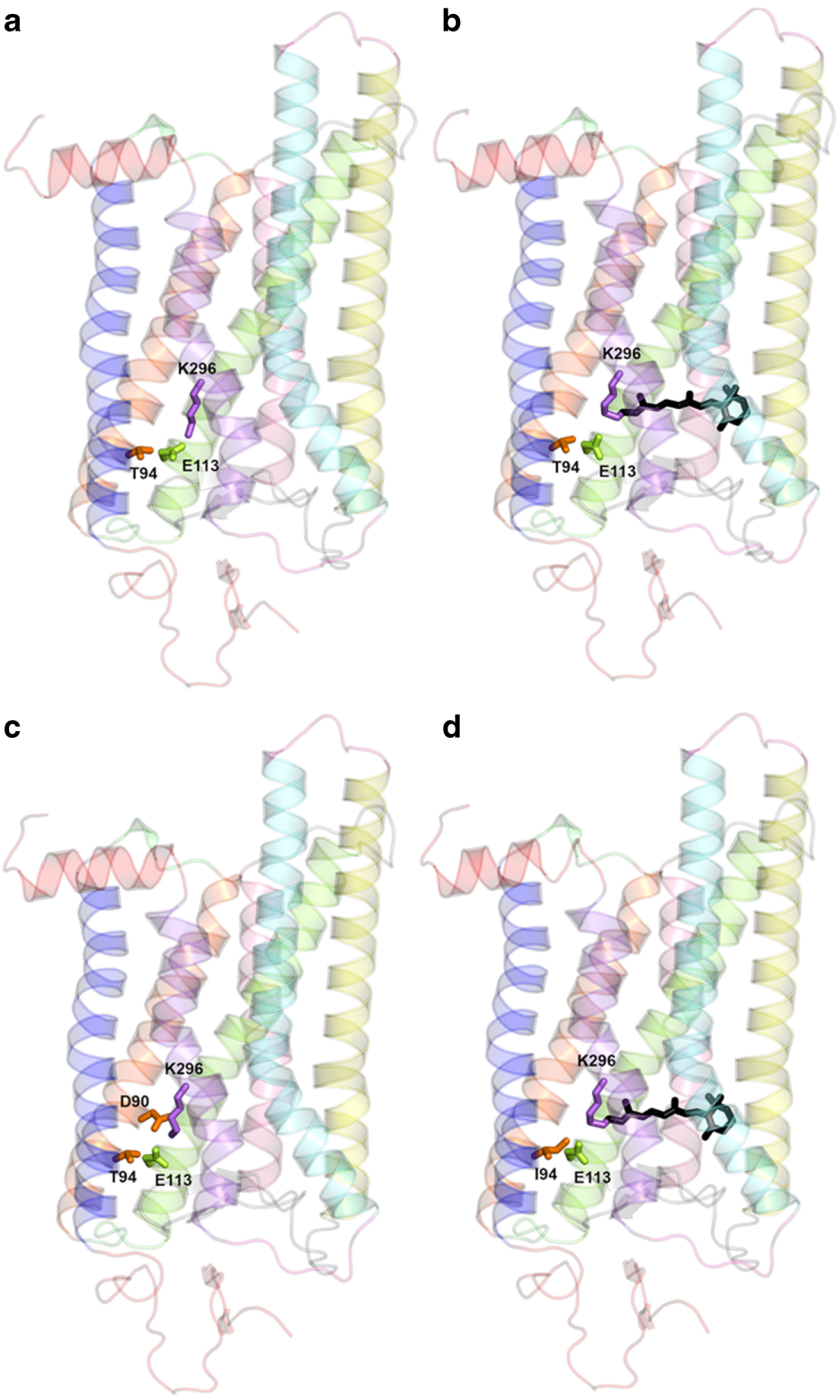

Fig. 7. Crystal structures of WT and CSNB mutant rod opsins. The crystal structures of WT Ops* (PDB: 3CAP [120]) (**a**), MII (PDB: 3PXO [24]) (**b**), D90D (PDB: 4BEZ [147]) (**c**), and T95I (PDB: 5DYS [146]) (**d**) are shown

would be the ability of both replacing amino acids in H2 to interact with K296(7.43), thus altering the dark state by weakening the interaction between the SB and its counterion E113(3.28) [146, 147].

Retinal dystrophies due to adRP *RHO* mutations represent a challenge in developing therapeutic intervention also because many of those mutations cause different degree of misfolding of the opsin protein. The inherent instability of those mutants impedes high-resolution structure determination. So far, atomic-level investigations relied on structural bioinformatics and molecular simulations.

The protein design algorithm FoldX was challenged to estimate the effects of adRP mutations on the stability of native rhodopsin [127]. In spite of the general usefulness of the tool, neglecting structural changes in free energy calculations makes the approach inadequate to estimate the effects of adRP rod opsin mutations that are linked to protein misfolding.

Understanding the molecular bases of conformational diseases requires the characterization of the interacting forces that drive folding, stabilize the native state, and, once impaired, lead to misfolding. We employed a number of computational strategies to face this issue. Replica exchange molecular dynamics (REMD) simulations served to investigate the effects of 40 rhodopsin mutations located in E2 on the conformation of the β-hairpin [39]. All the adRP *RHO* mutants in E2 were included in the simulated set. The free energy landscape of β-hairpin formation was found to align with in vitro mutational effects. Indeed, marked effects on the stability of E2 were exhibited only by those mutations causing severe impairments in folding/expression of the opsin protein [39]. Further insights were inferred from computational experiments based on the combination of mechanical unfolding simulations and protein structure network (PSN) analysis, an ever increasingly used approach to investigate structural communication, folding, and stability [36, 37, 164]. The study suggested that adRP misfolding *RHO* mutations tend to weaken a number of highly connected amino acids in the proximity to the retinal binding site and the G protein-binding regions [37].

In a more recent study, molecular simulations (i.e., 300K and melting unfolding simulations) coupled to the graph-based PSN analysis were combined with in vitro subcellular localization analyses to infer the effects of 33 adRP *RHO* mutations on stability and transport of the protein in the absence and presence of the retinal ligand [12].

The working hypothesis was that misfolded adRP mutants represent "quasi-native" states of the opsin protein.

While in silico experiments on the rhodopsin state employed 11-*cis*-retinal, present in the selected 1GZM structure, in vitro experiments employed 9-*cis*-retinal. The ability of 9-*cis*- and 11-*cis*-retinal to promote proper folding and trafficking has been previously demonstrated for the adRP mutants P23H, T17M, and Q28H [76, 82, 88, 99, 109, 110]. The employment of 9-*cis*-retinal in our subcellular localization analyses was dictated by the fact that the 9-*cis*-isomer is more stable than the 11-*cis*-isomer and shows similar behaviors, thus making it a good substitute [76, 117].

Remarkably, for both the opsin and rhodopsin states, a linear correlation was obtained between an index of structure network perturbation (NP) and the Pearson correlation coefficient (PCC) of calnexin/rhodopsin co-localization accounting for ER retention (i.e., the higher the PCC, the higher the co-localization between rod opsin and the ER-resident protein calnexin is [12]). Such a linear correlation between indices of misfolding and mislocalization allowed inferring common structural defects held by the mutants in relation to their ER retention.

The NP index served to divide the adRP *RHO* mutants into four clusters. Mutant clustering based upon the NP index computed on the opsin and rhodopsin states and the ΔNP was in line with ER retention [12]. In synthesis, mutant clusters 1 and 4 show, respectively, the lowest and highest destabilization of the native structure network and ER retention independent of the presence of retinal (i.e., either 11-*cis* or 9-*cis*), whereas cluster 2 resembles cluster 4 in the absence of retinal and cluster 1 in the presence of retinal. In other words, for cluster 2, the presence of retinal hinders structural impairment and mislocalization by mutation. The structural and cellular behaviors of cluster-3 mutants lie in between those of clusters 2 and 4 [12]. In this respect, cluster-1 mutants are T4K, M44T, F45L, G51A, T58R, G89D, G106R, L125R, V137M, A164V, and C167R; cluster-2 mutants are T17M, Q28H, V87D, R135W, P171Q, E181K, D190Y, and P267L; cluster-3 mutants are P23H, Y178C, P180A, S186P, and D190G; and cluster-4 mutants are L46R, P53R, C110Y, G114D, C187Y, G188R, H211P, H211R, and C222R.

The correlation between NP and PCC revealed a bridge between the classification of mutants based on their structural perturbation and the classification based on their ER retention [12]. Earlier classifications of adRP *RHO* mutants essentially relied on mutational effects on ER retention and the ability of rod opsin to bind retinal (reviewed in [18, 82]. Our in vitro data on mutant opsin agreed substantially with previous data on ER retention (reviewed in [18, 82]). Apparent discrepancies regard two mutants (L125R and C167R) assigned to classes IIb/II [18, 82, 151] and IIa/II [17, 18, 82, 154], respectively, but localized at the plasma membrane in our experiments and one mutant (L46R) assigned to class I [18] but retained in the ER in our experiments. As for L125R and C167R, molecular simulations showed that the replacing arginine makes a salt bridge with E122, which, consistent with poor ER retention and good plasma membrane targeting, does not perturb the native network in the opsin state. Simulations of C167R and L125R rhodopsin, however, showed that the replacing arginine, especially in L125R, induced deformations in the retinal ligand [12]. This may suggest that mutant opsins are able to reach plasma membrane even if impaired in retinal binding, consistent with L125R opsin showing WT-like electrophoretic pattern [47]. Thus for cluster-1 mutants, which reach plasma membrane and show low ER retention either in the opsin or rhodopsin states, the chaperone effect of the chromophore, if any, is masked. Therefore, our subcellular localization analysis could not distinguish cluster-1 mutants able to bind retinal from cluster-1 mutants unable to do so.

More discrepancies concern mutant responses to retinal, possibly due to divergences in the experimental approaches. Whereas previous studies employed spectroscopic analyses to evaluate rod opsin regeneration with retinal, we evaluated the ability of retinal to improve the subcellular localization of those mutants mostly retained into ER and not targeted to the plasma membrane in their opsin state. In our study, five (P171Q, Y178C, E181K, S186P, and D190Y) out of eleven (C110Y, G114D, P171Q, Y178C, E181K, S186P, C187Y,

D190Y, H211P, H211R, and C222R) mutants, previously found unable to reconstitute with retinal (i.e., falling in class IIa/II [2, 17, 18, 60, 62, 69, 71, 82, 131, 154, 166]), could instead improve their plasma membrane targeting and relieve ER retention as an effect of retinal binding.

By considering the adRP *RHO* mutant grouping into seven classes by Athanasiou and co-workers, while class 2 comprises possibly misfolded mutants because of their ER retention and impairment in retinal binding, the other classes comprise mutants thought to be properly folded but impaired in different aspects of rod opsin function [5]. Consistently, cluster-2, 3, and 4 mutants from our study, which are retained in the ER at least in their opsin form, fall into class 2. Consistency was also found for a number of mutants in our clusters 1 and 2, which fall in classes 3 (R135W [25]), 4 (T4K and T17M [22, 134, 157]), 5 (M44T and V137M [2]), and 7 (F45L [123]) by Athanasiou et al. and include also a mutant considered as a benign single-mutant polymorphism (G51A) [5]. Indeed, for those mutants showing membrane targeting at least in the presence of retinal, defects other than ER retention may cause the pathologic phenotype. In particular, (a) R135W is hyperphosphorylated and bound with high affinity to Arr1 [25]; (b) T4K and T17M, located in structured portions of the Nt, by affecting backbone conformation, may alter N-linked glycosylation [22, 134, 157]; (c) M44T and V137M were found to increase initial activation rates of transducin, though not bearing any constitutive activity [2]; and (d) F45L is expected to impair rod opsin dimerization [123]. Six mutants from our cluster 1 (T58R, G89D, G106R, L125R, A164V, and C167R) were ascribed to class-2 retinal non-responsive mutants by Athanasiou and co-workers [5, 17, 60, 130, 151, 154, 155]. In line with the statements above, cluster-1 mutants are poorly retained into ER and reach plasma membrane independent of retinal presence. Therefore, those mutants may be not retained into ER, consistent with our data, but impaired in retinal binding, consistent with mutant classification by Athanasiou and co-workers [5].

Early mass spectrometry determinations on four adRP mutants indicated partial (for G89D and A164V) or complete (for L125R and H211P) misfolding of rod opsin due to the formation of a non-native disulfide bridge between C185 and C187 in E2 [61]. Three of those mutants fall in our cluster 1, suggesting that, if present, such a non-native disulfide bridge would be compatible with a protein state targetable to the plasma membrane even in the absence of retinal.

Collectively, our investigation revealed some retinal responsiveness in 13 out of 22 adRP rod opsin mutants found retained into ER and not targeted to the plasma membrane in their opsin form. Those mutants may be target candidates of small chaperones recognizing the orthosteric retinal binding site. Remarkably, some cluster-1 mutants while not mislocalized may not respond to the retinal.

Effective structural signatures of each cluster, as inferred from the structure networks, were the native stable links that undergo an average frequency reduction ≥ 25% in the mutant trajectories belonging to the cluster (i.e., ≥ 40% frequency reduction in the perturbed networks shown in Fig. 8 a and b). By focusing on the intradiscal half of the receptor, which hosts the retinal binding site, it was observed that, in the opsin state, the lowest perturbation of native stable links concerns cluster 1 (Fig. 8b). Noticeably, 11-*cis*-retinal acts as a chaperone by preventing major link weakening shared in the opsin state by the mutants of cluster 1 and, more prominently, of clusters 2 and 3. In contrast, the ligand is less effective as a chaperone for clusters-4 mutants (Fig. 8b) [12]. Collectively, all mutants show marked link destabilization in the opsin state as an effect of mutation on protein structure and dynamics. Major structural differences among the four clusters concerned destabilization of native links in the intradiscal half of the receptor and in the ability of 11-*cis*-retinal to impede such perturbations, thus acting as a small chaperone. The structural effects of 11-*cis*-retinal were maximal for clusters 2 and 3 but minimal for cluster 4. The significant perturbation in the retinal binding site suggested that cluster-4 mutants are deficient in retinal binding in line with the inability of the retinal to relieve ER retention of mutant opsins.

The stability core of rod opsin inferred from the PSN analysis was targeted by virtual screening of over 300,000 anionic compounds, which led to the discovery of a novel chaperone, 5,8-epoxy-13-*cis* retinoic acid (13-*cis*-5,8-ERA), able to bind bovine opsin with 14-fold better EC_{50} (8.6 ± 0.2 nM) than 9-*cis*-retinal (123.9 ± 7.0 nM). Acting as a reversible orthosteric inhibitor of retinal binding, the compound proved more effective than 9-*cis*-retinal in promoting membrane localization of three adRP *RHO* mutants from the retinal-responsive clusters 2 and 3, i.e., T17M, P23H, and E181K [12]. In the same period, other two studies reported on the discovery of small chaperones able to bind bovine rod opsin and to promote membrane localization of P23H opsin though with EC_{50} comparable or worse than that of 9-*cis*-retinal [23, 95].

A recent extension of mechanical unfolding simulations coupled to PSN analysis to the same set of 33 adRP *RHO* mutants allowed us to develop a structure-based automated approach able to predict ER retention of novel adRP mutants and the ability of small chaperones to mitigate such ER retention with therapeutic implications (Felline et al. under review). In this framework, the average distributions of stable native hubs (i.e., nodes with at least four links) in the four clusters of mutants as a function of hub-link weakening and amino acid conservation provided valuable fingerprints of rhodopsin misfolding by mutation. Such fingerprints could distinguish mutants that do not respond to small chaperones from mutants either non-misfolded or responsive to small chaperones.

All these studies did not consider the tendency of partially misfolded mutants to aggregate with the WT as a possible determinant of the disease.

Collectively, thermal and mechanical unfolding simulations converge into the inference that misfolding rod opsin

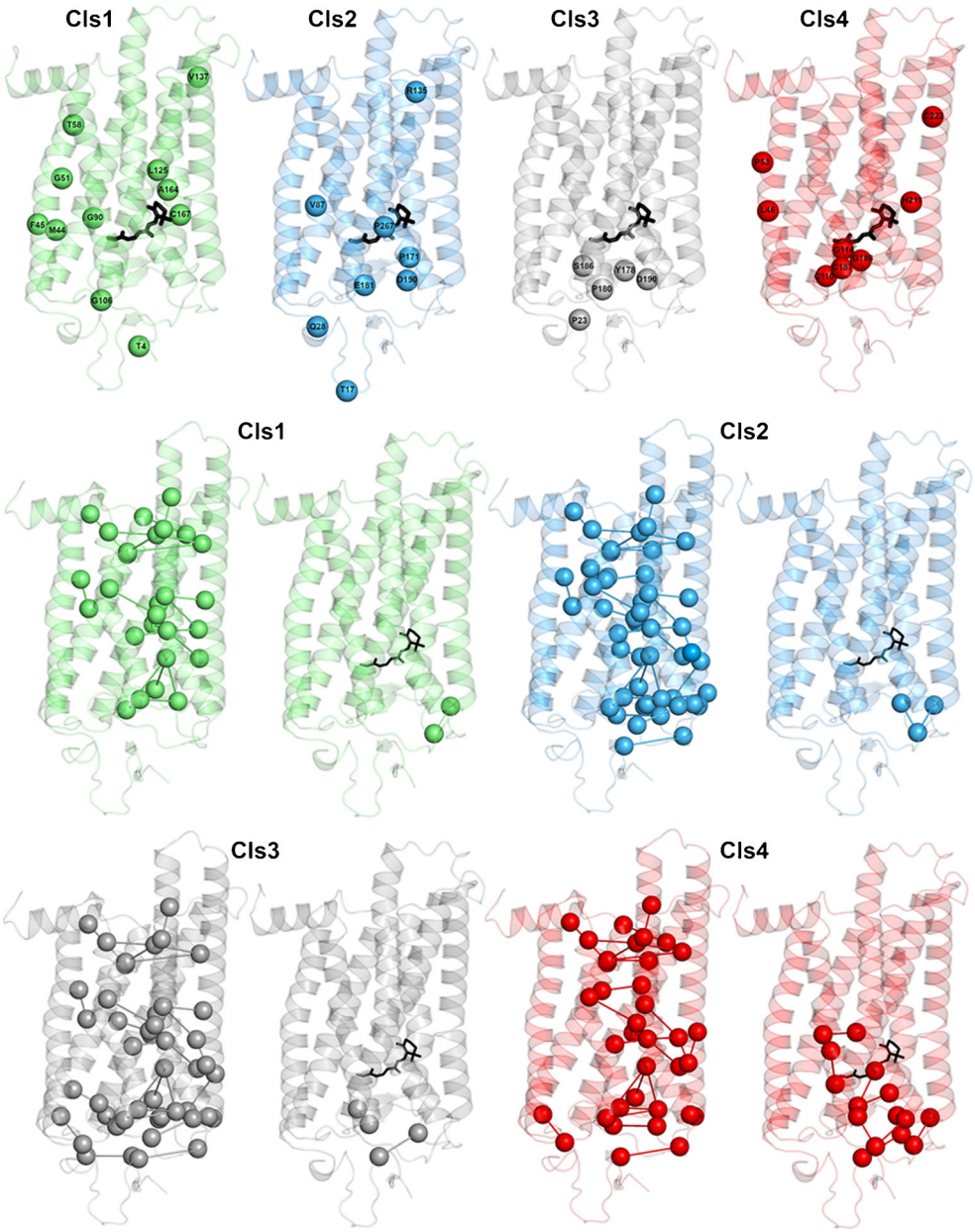

Fig. 8 Structural signatures of the four clusters of adRP mutants. **a** The mutation sites of the four clusters of mutants (clusters 1, 2, 3, and 4 are, respectively, light green, marine, gray, and red) are shown as spheres centered on the Cα-atoms. As already stated in the main text, cluster-1 mutants are T4K, M44T, F45L, G51A, T58R, G89D, G106R, L125R, V137M, A164V, and C167R; cluster-2 mutants are T17M, Q28H, V87D, R135W, P171Q, E181K, D190Y, and P267L; cluster-3 mutants are P23H, Y178C, P180A, S186P, and D190G; and cluster-4 mutants are L46R, P53R, C110Y, G114D, C187Y, G188R, H211P, H211R, and C222R

mutants weaken the stability core of the protein, which is participated by amino acids in the retinal binding site. The effects of such perturbations on the secondary structure elements and their spatial arrangements still remain undefined.

Conclusions and perspectives

Vertebrate rod opsin is the GPCR best characterized at the atomic level of detail. Since the release of the first crystal structure 20 years ago, a huge number of structures have been released that, in combination with valuable spectroscopic determinations, unveiled most aspects of the photobleaching process.

Retinal dystrophies due to adRP *RHO* mutations still represent a challenge because the inherent instability of such mutants so far impeded high-resolution structure determinations.

The existent structures of WT rod opsin in its apo and retinal-bound forms were exploited as input structures for unfolding simulations and analysis of adRP *RHO* mutants with valuable hints. Those simulations, indeed, converged into the inference that misfolding rod opsin mutations weaken the stability core of the protein, which is participated by amino acids in the retinal binding site. The effects of such perturbations on the secondary structure elements and their architecture still remain undefined. The ability of some misfolded mutants to aggregate with the WT as a possible determinant

of the disease awaits elucidation as well. The combination of in silico and in vivo experiments suggest that at least all mutants in clusters 1, 2, and 3 are in quasi-native states and that mutants from clusters 2 and 3 are recovered by small chaperones like 11-*cis*-retinal and 13-*cis*-5,8-ERA.

As already shown, a computational approach based on the combination of misfolding simulations of rod opsin mutants with PSN analysis and virtual screening of compounds targeting the stability core of the protein may lead to the discovery of small chaperones, even better than the one discovered so far. This would have important implications in personalized therapeutic interventions for adRP linked to rod opsin mutations. Actually, our efforts are going in that direction.

Acknowledgements Drawings were done by means of the software PYMOL 1.1r1 (http://pymol.sourceforge.net/). We thank Krzysztof Palczewski for providing the coordinates of the latest rhodopsin oligomeric structural model.

Funding This study was supported by a Telethon-Italy grant [GGP11210], by a Fondazione Roma grant (call for proposals 2013 on Retinitis Pigmentosa), and by a FAR2018 grant to both FF and VM.

Data availability Not applicable.

Declarations

Consent for publication The authors give consent to publish.

Conflict of interest The authors declare no competing interests.

References

1. Aguila M, Bevilacqua D, McCulley C, Schwarz N, Athanasiou D, Kanuga N, Novoselov SS, Lange CA, Ali RR, Bainbridge JW, Gias C, Coffey PJ, Garriga P, Cheetham ME (2014) Hsp90 inhibition protects against inherited retinal degeneration. Hum Mol Genet 23:2164–2175. https://doi.org/10.1093/hmg/ddt613
2. Andres A, Garriga P, Manyosa J (2003) Altered functionality in rhodopsin point mutants associated with retinitis pigmentosa. Biochem Biophys Res Commun 303:294–301
3. Arnis S, Hofmann KP (1993) Two different forms of metarhodopsin II: Schiff base deprotonation precedes proton uptake and signaling state. Proc Natl Acad Sci U S A 90:7849–7853
4. Arvanitakis L, Geras-Raaka E, Gershengorn MC (1998) Constitutively signaling G-protein coupled receptor and human disease. Trends Endocrinol Metab 9:27–31
5. Athanasiou D, Aguila M, Bellingham J, Li WW, McCulley C, Reeves PJ, Cheetham ME (2018) The molecular and cellular basis of rhodopsin retinitis pigmentosa reveals potential strategies for therapy. Prog Retin Eye Res 62:1–23. https://doi.org/10.1016/j.preteyeres.2017.10.002
6. Baldwin JM (1993) The probable arrangement of the helices in G protein-coupled receptors. EMBO J 12:1693–1703
7. Baldwin JM, Schertler GF, Unger VM (1997) An alpha-carbon template for the transmembrane helices in the rhodopsin family of G-protein-coupled receptors. J Mol Biol 272:144–164
8. Ballesteros JA, Weinstein H (1995) Integrated methods for the construction of three-dimensional models and computational probing of structure-function relations in G protein-coupled receptors. Methods Neurosci 25:366–428
9. Bartl FJ, Ritter E, Hofmann KP (2001) Signaling states of rhodopsin: absorption of light in active metarhodopsin II generates an all-trans-retinal bound inactive state. J Biol Chem 276:30161–30166
10. Bayburt TH, Leitz AJ, Xie G, Oprian DD, Sligar SG (2007) Transducin activation by nanoscale lipid bilayers containing one and two rhodopsins. J Biol Chem 282:14875–14881. https://doi.org/10.1074/jbc.M701433200
11. Baylor D (1996) How photons start vision. Proc Natl Acad Sci U S A 93:560–565
12. Behnen P, Felline A, Comitato A, Di Salvo MT, Raimondi F, Gulati S, Kahremany S, Palczewski K, Marigo V, Fanelli F (2018) A small chaperone improves folding and routing of rhodopsin mutants linked to inherited blindness. iScience 4:1–19
13. Blankenship E, Vahedi-Faridi A, Lodowski DT (2015) The high-resolution structure of activated opsin reveals a conserved solvent network in the transmembrane region essential for activation. Structure 23:2358–2364. https://doi.org/10.1016/j.str.2015.09.015
14. Bockaert J, Pin JP (1999) Molecular tinkering of G protein-coupled receptors: an evolutionary success. EMBO J 18:1723–1729
15. Bouvier M (2001) Oligomerization of G-protein-coupled transmitter receptors. Nat Rev Neurosci 2:274–286
16. Brady AE, Limbird LE (2002) G protein-coupled receptor interacting proteins: emerging roles in localization and signal transduction. Cell Signal 14:297–309
17. Breikers G, Portier-VandeLuytgaarden MJ, Bovee-Geurts PH, DeGrip WJ (2002) Retinitis pigmentosa-associated rhodopsin mutations in three membrane-located cysteine residues present three different biochemical phenotypes. Biochem Biophys Res Commun 297:847–853
18. Briscoe AD, Gaur C, Kumar S (2004) The spectrum of human rhodopsin disease mutations through the lens of interspecific variation. Gene 332:107–118. https://doi.org/10.1016/j.gene.2004.02.037
19. Chabre M, Cone R, Saibil H (2003) Biophysics: is rhodopsin dimeric in native retinal rods? Nature 426:30–31 discussion 31
20. Chabre M, Deterre P, Antonny B (2009) The apparent cooperativity of some GPCRs does not necessarily imply dimerization. Trends Pharmacol Sci 30:182–187. https://doi.org/10.1016/j.tips.2009.01.003
21. Chabre M, le Maire M (2005) Monomeric G-protein-coupled receptor as a functional unit. Biochemistry 44:9395–9403
22. Chen Y, Jastrzebska B, Cao P, Zhang J, Wang B, Sun W, Yuan Y, Feng Z, Palczewski K (2014) Inherent instability of the retinitis pigmentosa P23H mutant opsin. J Biol Chem 289:9288–9303. https://doi.org/10.1074/jbc.M114.551713
23. Chen YY, Chen Y, Jastrzebska B, Golczak M, Gulati S, Tang H, Seibel W, Li XYY, Jin H, Han Y, Gao SQ, Zhang JY, Liu XJ, Heidari-Torkabadi H, Stewart PL, Harte WE, Tochtrop GP, Palczewski K (2018) A novel small molecule chaperone of rod opsin and its potential therapy for retinal degeneration. Nat Commun 9. 1976 https://doi.org/10.1038/S41467-018-04261-1
24. Choe HW, Kim YJ, Park JH, Morizumi T, Pai EF, Krauss N, Hofmann KP, Scheerer P, Ernst OP (2011) Crystal structure of metarhodopsin II. Nature 471:651–655. https://doi.org/10.1038/nature09789
25. Chuang JZ, Vega C, Jun W, Sung CH (2004) Structural and functional impairment of endocytic pathways by retinitis pigmentosa mutant rhodopsin-arrestin complexes. J Clin Invest 114:131–140
26. Cohen GB, Yang T, Robinson PR, Oprian DD (1993) Constitutive activation of opsin: influence of charge at position 134 and size at position 296. Biochemistry 32:6111–6115

27. Conn PM, Ulloa-Aguirre A (2010) Trafficking of G-protein-coupled receptors to the plasma membrane: insights for pharmacoperone drugs. Trends Endocrinol Metab 21:190–197. https://doi.org/10.1016/j.tem.2009.11.003
28. Costa T, Cotecchia S (2005) Historical review: negative efficacy and the constitutive activity of G-protein-coupled receptors. Trends Pharmacol Sci 26:618–624. https://doi.org/10.1016/j.tips.2005.10.009
29. Dell'Orco D, Koch KW (2015) Transient complexes between dark rhodopsin and transducin: circumstantial evidence or physiological necessity? Biophys J 108:775–777. https://doi.org/10.1016/j.bpj.2014.12.031
30. Dell'Orco D, Schmidt H, Mariani S, Fanelli F (2009) Network-level analysis of light adaptation in rod cells under normal and altered conditions. Mol BioSyst 5:1232–1246. https://doi.org/10.1039/b908123b
31. Deupi X, Edwards P, Singhal A, Nickle B, Oprian D, Schertler G, Standfuss J (2012) Stabilized G protein binding site in the structure of constitutively active metarhodopsin-II. Proc Natl Acad Sci U S A 109:119–124. https://doi.org/10.1073/pnas.1114089108
32. Dizhoor AM, Woodruff ML, Olshevskaya EV, Cilluffo MC, Cornwall MC, Sieving PA, Fain GL (2008) Night blindness and the mechanism of constitutive signaling of mutant G90D rhodopsin. J Neurosci 28:11662–11672. https://doi.org/10.1523/JNEUROSCI.4006-08.2008
33. Ernst OP, Gramse V, Kolbe M, Hofmann KP, Heck M (2007) Monomeric G protein-coupled receptor rhodopsin in solution activates its G protein transducin at the diffusion limit. Proc Natl Acad Sci U S A 104:10859–10864
34. Fahmy K, Sakmar TP, Siebert F (2000) Transducin-dependent protonation of glutamic acid 134 in rhodopsin. Biochemistry 39:10607–10612
35. Fanelli F, De Benedetti PG (2011) Update 1 of: computational modeling approaches to structure-function analysis of G protein-coupled receptors. Chem Rev 111:PR438–PR535. https://doi.org/10.1021/cr100437t
36. Fanelli F, Felline A, Raimondi F (2013) Network analysis to uncover the structural communication in GPCRs. Methods Cell Biol 117:43–61. https://doi.org/10.1016/B978-0-12-408143-7.00003-7
37. Fanelli F, Seeber M (2010) Structural insights into retinitis pigmentosa from unfolding simulations of rhodopsin mutants. FASEB J 24:3196–3209. https://doi.org/10.1096/fj.09-151084
38. Farrens DL, Khorana HG (1995) Structure and function in rhodopsin. Measurement of the rate of metarhodopsin II decay by fluorescence spectroscopy. J Biol Chem 270:5073–5076
39. Felline A, Seeber M, Rao F, Fanelli F (2009) Computational screening of rhodopsin mutations associated with retinitis pigmentosa. J Chem Theory Comput 5:2472–2485. https://doi.org/10.1021/Ct900145u
40. Ferrari S, Di Iorio E, Barbaro V, Ponzin D, Sorrentino FS, Parmeggiani F (2011) Retinitis pigmentosa: genes and disease mechanisms. Curr Genom 12:238–249
41. Flock T, Ravarani CN, Sun D, Venkatakrishnan AJ, Kayikci M, Tate CG, Veprintsev DB, Babu MM (2015) Universal allosteric mechanism for Galpha activation by GPCRs. Nature 524:173–179. https://doi.org/10.1038/nature14663
42. Fotiadis D, Jastrzebska B, Philippsen A, Muller DJ, Palczewski K, Engel A (2006) Structure of the rhodopsin dimer: a working model for G-protein-coupled receptors. Curr Opin Struct Biol 16:252–259
43. Fotiadis D, Liang Y, Filipek S, Saperstein DA, Engel A, Palczewski K (2003) Atomic-force microscopy: rhodopsin dimers in native disc membranes. Nature 421:127–128
44. Fotiadis D, Liang Y, Filipek S, Saperstein DA, Engel A, Palczewski K (2004) The G protein-coupled receptor rhodopsin in the native membrane. FEBS Lett 564:281–288
45. Frins S, Bonigk W, Muller F, Kellner R, Koch KW (1996) Functional characterization of a guanylyl cyclase-activating protein from vertebrate rods. Cloning, heterologous expression, and localization. J Biol Chem 271:8022–8027
46. Gao Y, Hu H, Ramachandran S, Erickson JW, Cerione RA, Skiniotis G (2019) Structures of the rhodopsin-transducin complex: insights into G-protein activation. Mol Cell 75:781–790 e783. https://doi.org/10.1016/j.molcel.2019.06.007
47. Garriga P, Liu X, Khorana HG (1996) Structure and function in rhodopsin: correct folding and misfolding in point mutants at and in proximity to the site of the retinitis pigmentosa mutation Leu-125–>Arg in the transmembrane helix C. Proc Natl Acad Sci U S A 93:4560–4564. https://doi.org/10.1073/pnas.93.10.4560
48. Gether U (2000) Uncovering molecular mechanisms involved in activation of G protein-coupled receptors. Endocr Rev 21:90–113
49. Goricanec D, Stehle R, Egloff P, Grigoriu S, Pluckthun A, Wagner G, Hagn F (2016) Conformational dynamics of a G-protein alpha subunit is tightly regulated by nucleotide binding. Proc Natl Acad Sci U S A 113:E3629–E3638. https://doi.org/10.1073/pnas.1604125113
50. Gragg M, Kim TG, Howell S, Park PS (2016) Wild-type opsin does not aggregate with a misfolded opsin mutant. Biochim Biophys Acta 1858:1850–1859. https://doi.org/10.1016/j.bbamem.2016.04.013
51. Gragg M, Park PS (2018) Misfolded rhodopsin mutants display variable aggregation properties. Biochim Biophys Acta Mol basis Dis 1864:2938–2948. https://doi.org/10.1016/j.bbadis.2018.06.004
52. Gragg M, Park PS (2019) Detection of misfolded rhodopsin aggregates in cells by Forster resonance energy transfer. Methods Cell Biol 149:87–105. https://doi.org/10.1016/bs.mcb.2018.08.007
53. Gulati S, Jastrzebska B, Banerjee S, Placeres AL, Miszta P, Gao SQ, Gunderson K, Tochtrop GP, Filipek S, Katayama K, Kiser PD, Mogi M, Stewart PL, Palczewski K (2017) Photocyclic behavior of rhodopsin induced by an atypical isomerization mechanism. Proc Natl Acad Sci U S A 114:E2608–E2615. https://doi.org/10.1073/pnas.1617446114
54. Hartong DT, Berson EL, Dryja TP (2006) Retinitis pigmentosa. Lancet 368:1795–1809. https://doi.org/10.1016/S0140-6736(06)69740-7
55. Heck M, Schadel SA, Maretzki D, Bartl FJ, Ritter E, Palczewski K, Hofmann KP (2003) Signaling states of rhodopsin. Formation of the storage form, metarhodopsin III, from active metarhodopsin II. J Biol Chem 278:3162–3169
56. Heck M, Schadel SA, Maretzki D, Hofmann KP (2003) Secondary binding sites of retinoids in opsin: characterization and role in regeneration. Vis Res 43:3003–3010
57. Hilger D, Masureel M, Kobilka BK (2018) Structure and dynamics of GPCR signaling complexes. Nat Struct Mol Biol 25:4–12. https://doi.org/10.1038/s41594-017-0011-7
58. Hirsch JA, Schubert C, Gurevich VV, Sigler PB (1999) The 2.8 A crystal structure of visual arrestin: a model for arrestin's regulation. Cell 97:257–269. https://doi.org/10.1016/s0092-8674(00)80735-7
59. Hofmann KP, Scheerer P, Hildebrand PW, Choe HW, Park JH, Heck M, Ernst OP (2009) A G protein-coupled receptor at work: the rhodopsin model. Trends Biochem Sci 34:540–552. https://doi.org/10.1016/j.tibs.2009.07.005
60. Hwa J, Garriga P, Liu X, Khorana HG (1997) Structure and function in rhodopsin: packing of the helices in the transmembrane domain and folding to a tertiary structure in the intradiscal domain are coupled. Proc Natl Acad Sci U S A 94:10571–10576

61. Hwa J, Klein-Seetharaman J, Khorana HG (2001) Structure and function in rhodopsin: mass spectrometric identification of the abnormal intradiscal disulfide bond in misfolded retinitis pigmentosa mutants. Proc Natl Acad Sci U S A 98:4872–4876. https://doi.org/10.1073/pnas.061632798
62. Hwa J, Reeves PJ, Klein-Seetharaman J, Davidson F, Khorana HG (1999) Structure and function in rhodopsin: further elucidation of the role of the intradiscal cysteines, Cys-110, -185, and -187, in rhodopsin folding and function. Proc Natl Acad Sci U S A 96:1932–1935
63. Jaeger K, Bruenle S, Weinert T, Guba W, Muehle J, Miyazaki T, Weber M, Furrer A, Haenggi N, Tetaz T, Huang CY, Mattle D, Vonach JM, Gast A, Kuglstatter A, Rudolph MG, Nogly P, Benz J, Dawson RJP, Standfuss J (2019) Structural basis for allosteric ligand recognition in the human CC chemokine receptor 7. Cell 178:1222–1230 e1210. https://doi.org/10.1016/j.cell.2019.07.028
64. Jastrzebska B, Fotiadis D, Jang GF, Stenkamp RE, Engel A, Palczewski K (2006) Functional and structural characterization of rhodopsin oligomers. J Biol Chem 281:11917–11922. https://doi.org/10.1074/jbc.M600422200
65. Jastrzebska B, Maeda T, Zhu L, Fotiadis D, Filipek S, Engel A, Stenkamp RE, Palczewski K (2004) Functional characterization of rhodopsin monomers and dimers in detergents. J Biol Chem 279:54663–54675
66. Jin S, Cornwall MC, Oprian DD (2003) Opsin activation as a cause of congenital night blindness. Nat Neurosci 6:731–735. https://doi.org/10.1038/nn1070
67. Kang Y, Zhou XE, Gao X, He Y, Liu W, Ishchenko A, Barty A, White TA, Yefanov O, Han GW, Xu Q, de Waal PW, Ke J, Tan MH, Zhang C, Moeller A, West GM, Pascal BD, Van Eps N, Caro LN, Vishnivetskiy SA, Lee RJ, Suino-Powell KM, Gu X, Pal K, Ma J, Zhi X, Boutet S, Williams GJ, Messerschmidt M, Gati C, Zatsepin NA, Wang D, James D, Basu S, Roy-Chowdhury S, Conrad CE, Coe J, Liu H, Lisova S, Kupitz C, Grotjohann I, Fromme R, Jiang Y, Tan M, Yang H, Li J, Wang M, Zheng Z, Li D, Howe N, Zhao Y, Standfuss J, Diederichs K, Dong Y, Potter CS, Carragher B, Caffrey M, Jiang H, Chapman HN, Spence JC, Fromme P, Weierstall U, Ernst OP, Katritch V, Gurevich VV, Griffin PR, Hubbell WL, Stevens RC, Cherezov V, Melcher K, Xu HE (2015) Crystal structure of rhodopsin bound to arrestin by femtosecond X-ray laser. Nature 523:561–567. https://doi.org/10.1038/nature14656
68. Kang YY, Kuybeda O, de Waal PW, Mukherjee S, Van Eps N, Dutka P, Zhou XE, Bartesaghi A, Erramilli S, Morizumi T, Gu X, Yin YT, Liu P, Jiang Y, Meng X, Zhao GP, Melcher K, Ernst OP, Kossiakoff AA, Subramaniam S, Xu HE (2018) Cryo-EM structure of human rhodopsin bound to an inhibitory G protein. Nature 558:553. https://doi.org/10.1038/s41586-018-0215-y
69. Karnik SS, Sakmar TP, Chen HB, Khorana HG (1988) Cysteine residues 110 and 187 are essential for the formation of correct structure in bovine rhodopsin. Proc Natl Acad Sci U S A 85:8459–8463
70. Katritch V, Cherezov V, Stevens RC (2013) Structure-function of the G protein-coupled receptor superfamily. Annu Rev Pharmacol Toxicol 53:531–556. https://doi.org/10.1146/annurev-pharmtox-032112-135923
71. Kaushal S, Khorana HG (1994) Structure and function in rhodopsin. 7. Point mutations associated with autosomal dominant retinitis pigmentosa. Biochemistry 33:6121–6128
72. Kefalov VJ, Crouch RK, Cornwall MC (2001) Role of noncovalent binding of 11-cis-retinal to opsin in dark adaptation of rod and cone photoreceptors. Neuron 29:749–755. https://doi.org/10.1016/s0896-6273(01)00249-5
73. Kennan A, Aherne A, Humphries P (2005) Light in retinitis pigmentosa. Trends Genet 21:103–110
74. Kim TH, Chung KY, Manglik A, Hansen AL, Dror RO, Mildorf TJ, Shaw DE, Kobilka BK, Prosser RS (2013) The role of ligands on the equilibria between functional states of a G protein-coupled receptor. J Am Chem Soc 135:9465–9474. https://doi.org/10.1021/ja404305k
75. Kim YJ, Hofmann KP, Ernst OP, Scheerer P, Choe HW, Sommer ME (2013) Crystal structure of pre-activated arrestin p44. Nature 497:142–146. https://doi.org/10.1038/nature12133
76. Kiser PD, Golczak M, Palczewski K (2014) Chemistry of the retinoid (visual) cycle. Chem Rev 114:194–232. https://doi.org/10.1021/cr400107q
77. Kliger DS, Lewis JW (1995) Spectral and kinetic characterization of visual pigment photointermediates. Israel J Chem 35:289–307
78. Knierim B, Hofmann KP, Ernst OP, Hubbell WL (2007) Sequence of late molecular events in the activation of rhodopsin. Proc Natl Acad Sci U S A 104:20290–20295. https://doi.org/10.1073/pnas.0710393104
79. Koch KW, Duda T, Sharma RK (2002) Photoreceptor specific guanylate cyclases in vertebrate phototransduction. Mol Cell Biochem 230:97–106
80. Kono M, Goletz PW, Crouch RK (2008) 11-cis- and all-trans-retinols can activate rod opsin: rational design of the visual cycle. Biochemistry 47:7567–7571. https://doi.org/10.1021/bi800357b
81. Kota P, Reeves PJ, Rajbhandary UL, Khorana HG (2006) Opsin is present as dimers in COS1 cells: identification of amino acids at the dimeric interface. Proc Natl Acad Sci U S A 103:3054–3059. https://doi.org/10.1073/pnas.0510982103
82. Krebs MP, Holden DC, Joshi P, Clark CL 3rd, Lee AH, Kaushal S (2010) Molecular mechanisms of rhodopsin retinitis pigmentosa and the efficacy of pharmacological rescue. J Mol Biol 395:1063–1078. https://doi.org/10.1016/j.jmb.2009.11.015
83. Kristiansen K (2004) Molecular mechanisms of ligand binding, signaling, and regulation within the superfamily of G-protein-coupled receptors: molecular modeling and mutagenesis approaches to receptor structure and function. Pharmacol Ther 103:21–80
84. Lamb TD (1996) Gain and kinetics of activation in the G-protein cascade of phototransduction. Proc Natl Acad Sci U S A 93:566–570
85. Lefkowitz RJ (2000) The superfamily of heptahelical receptors. Nat Cell Biol 2:E133–E136
86. Lefkowitz RJ, Cotecchia S, Samama P, Costa T (1993) Constitutive activity of receptors coupled to guanine nucleotide regulatory proteins. Trends Pharmacol Sci 14:303–307
87. Li J, Edwards PC, Burghammer M, Villa C, Schertler GF (2004) Structure of bovine rhodopsin in a trigonal crystal form. J Mol Biol 343:1409–1438
88. Li T, Sandberg MA, Pawlyk BS, Rosner B, Hayes KC, Dryja TP, Berson EL (1998) Effect of vitamin A supplementation on rhodopsin mutants threonine-17 –> methionine and proline-347 –> serine in transgenic mice and in cell cultures. Proc Natl Acad Sci U S A 95:11933–11938
89. Liang Y, Fotiadis D, Filipek S, Saperstein DA, Palczewski K, Engel A (2003) Organization of the G protein-coupled receptors rhodopsin and opsin in native membranes. J Biol Chem 278:21655–21662
90. Lin JC, Liu HL (2006) Protein conformational diseases: from mechanisms to drug designs. Curr Drug Discov Technol 3:145–153
91. Lin JH, Li H, Yasumura D, Cohen HR, Zhang C, Panning B, Shokat KM, Lavail MM, Walter P (2007) IRE1 signaling affects cell fate during the unfolded protein response. Science 318:944–949. https://doi.org/10.1126/science.1146361
92. Lodowski DT, Salom D, Le Trong I, Teller DC, Ballesteros JA, Palczewski K, Stenkamp RE (2007) Crystal packing analysis of

Rhodopsin crystals. J Struct Biol 158:455–462. https://doi.org/10.1016/j.jsb.2007.01.017
93. Lohse MJ (2010) Dimerization in GPCR mobility and signaling. Curr Opin Pharmacol 10:53–58. https://doi.org/10.1016/j.coph.2009.10.007
94. Makino CL, Riley CK, Looney J, Crouch RK, Okada T (2010) Binding of more than one retinoid to visual opsins. Biophys J 99:2366–2373. https://doi.org/10.1016/j.bpj.2010.08.003
95. Mattle D, Kuhn B, Aebi J, Bedoucha M, Kekilli D, Grozinger N, Alker A, Rudolph MG, Schmid G, Schertler GFX, Hennig M, Standfuss J, Dawson RJP (2018) Ligand channel in pharmacologically stabilized rhodopsin. Proc Natl Acad Sci U S A 115:3640–3645. https://doi.org/10.1073/pnas.1718084115
96. McAlear SD, Kraft TW, Gross AK (2010) 1 rhodopsin mutations in congenital night blindness. Adv Exp Med Biol 664:263–272. https://doi.org/10.1007/978-1-4419-1399-9_30
97. McBee JK, Palczewski K, Baehr W, Pepperberg DR (2001) Confronting complexity: the interlink of phototransduction and retinoid metabolism in the vertebrate retina. Prog Retin Eye Res 20:469–529
98. Melia TJ Jr, Cowan CW, Angleson JK, Wensel TG (1997) A comparison of the efficiency of G protein activation by ligand-free and light-activated forms of rhodopsin. Biophys J 73:3182–3191
99. Mendes HF, Cheetham ME (2008) Pharmacological manipulation of gain-of-function and dominant-negative mechanisms in rhodopsin retinitis pigmentosa. Hum Mol Genet 17:3043–3054. https://doi.org/10.1093/hmg/ddn202
100. Mendes HF, van der Spuy J, Chapple JP, Cheetham ME (2005) Mechanisms of cell death in rhodopsin retinitis pigmentosa: implications for therapy. Trends Mol Med 11:177–185
101. Milligan G (2010) The role of dimerisation in the cellular trafficking of G-protein-coupled receptors. Curr Opin Pharmacol 10:23–29. https://doi.org/10.1016/j.coph.2009.09.010
102. Mirzadegan T, Benko G, Filipek S, Palczewski K (2003) Sequence analyses of G-protein-coupled receptors: similarities to rhodopsin. Biochemistry 42:2759–2767
103. Mishra AK, Gragg M, Stoneman MR, Biener G, Oliver JA, Miszta P, Filipek S, Raicu V, Park PS (2016) Quaternary structures of opsin in live cells revealed by FRET spectrometry. Biochem J 473:3819–3836. https://doi.org/10.1042/BCJ20160422
104. Nakamichi H, Buss V, Okada T (2007) Photoisomerization mechanism of rhodopsin and 9-cis-rhodopsin revealed by X-ray crystallography. Biophys J 92:L106–L108. https://doi.org/10.1529/biophysj.107.108225
105. Nakamichi H, Okada T (2006) Crystallographic analysis of primary visual photochemistry. Angew Chem Int Ed Eng 45:4270–4273. https://doi.org/10.1002/anie.200600595
106. Nakamichi H, Okada T (2006) Local peptide movement in the photoreaction intermediate of rhodopsin. Proc Natl Acad Sci U S A 103:12729–12734. https://doi.org/10.1073/pnas.0601765103
107. Nakamichi H, Okada T (2007) X-ray crystallographic analysis of 9-cis-rhodopsin, a model analogue visual pigment. Photochem Photobiol 83:232–235. https://doi.org/10.1562/2006-13-Ra-920
108. Noel JP, Hamm HE, Sigler PB (1993) The 2.2 A crystal structure of transducin-alpha complexed with GTP gamma S. Nature 366:654–663. https://doi.org/10.1038/366654a0
109. Noorwez SM, Malhotra R, McDowell JH, Smith KA, Krebs MP, Kaushal S (2004) Retinoids assist the cellular folding of the autosomal dominant retinitis pigmentosa opsin mutant P23H. J Biol Chem 279:16278–16284. https://doi.org/10.1074/jbc.M312101200
110. Noorwez SM, Sama RR, Kaushal S (2009) Calnexin improves the folding efficiency of mutant rhodopsin in the presence of pharmacological chaperone 11-cis-retinal. J Biol Chem 284:33333–33342. https://doi.org/10.1074/jbc.M109.043364
111. Okada T, Ernst OP, Palczewski K, Hofmann KP (2001) Activation of rhodopsin: new insights from structural and biochemical studies. Trends Biochem Sci 26:318–324
112. Okada T, Fujiyoshi Y, Silow M, Navarro J, Landau EM, Shichida Y (2002) Functional role of internal water molecules in rhodopsin revealed by X-ray crystallography. Proc Natl Acad Sci U S A 99:5982–5987
113. Okada T, Sugihara M, Bondar AN, Elstner M, Entel P, Buss V (2004) The retinal conformation and its environment in rhodopsin in light of a new 2.2 A crystal structure. J Mol Biol 342:571–583
114. Palczewski K (1997) GTP-binding-protein-coupled receptor kinases–two mechanistic models. Eur J Biochem 248:261–269
115. Palczewski K (2006) G protein-coupled receptor rhodopsin. Annu Rev Biochem 75:743–767. https://doi.org/10.1146/annurev.biochem.75.103004.142743
116. Palczewski K (2010) Oligomeric forms of G protein-coupled receptors (GPCRs). Trends Biochem Sci 35:595–600. https://doi.org/10.1016/j.tibs.2010.05.002
117. Palczewski K (2010) Retinoids for treatment of retinal diseases. Trends Pharmacol Sci 31:284–295. https://doi.org/10.1016/j.tips.2010.03.001
118. Palczewski K, Kumasaka T, Hori T, Behnke CA, Motoshima H, Fox BA, Le Trong I, Teller DC, Okada T, Stenkamp RE, Yamamoto M, Miyano M (2000) Crystal structure of rhodopsin: a G protein-coupled receptor. Science 289:739–745
119. Park JH, Morizumi T, Li Y, Hong JE, Pai EF, Hofmann KP, Choe HW, Ernst OP (2013) Opsin, a structural model for olfactory receptors? Angew Chem Int Ed Eng 52:11021–11024. https://doi.org/10.1002/anie.201302374
120. Park JH, Scheerer P, Hofmann KP, Choe HW, Ernst OP (2008) Crystal structure of the ligand-free G-protein-coupled receptor opsin. Nature 454:183–187. https://doi.org/10.1038/nature07063
121. Park PS, Filipek S, Wells JW, Palczewski K (2004) Oligomerization of G protein-coupled receptors: past, present, and future. Biochemistry 43:15643–15656
122. Pierce KL, Premont RT, Lefkowitz RJ (2002) Seven-transmembrane receptors. Nat Rev Mol Cell Biol 3:639–650
123. Ploier B, Caro LN, Morizumi T, Pandey K, Pearring JN, Goren MA, Finnemann SC, Graumann J, Arshavsky VY, Dittman JS, Ernst OP, Menon AK (2016) Dimerization deficiency of enigmatic retinitis pigmentosa-linked rhodopsin mutants. Nat Commun 7:12832. https://doi.org/10.1038/ncomms12832
124. Pulvermuller A, Palczewski K, Hofmann KP (1993) Interaction between photoactivated rhodopsin and its kinase: stability and kinetics of complex formation. Biochemistry 32:14082–14088
125. Punzo C, Kornacker K, Cepko CL (2009) Stimulation of the insulin/mTOR pathway delays cone death in a mouse model of retinitis pigmentosa. Nat Neurosci 12:44–52. https://doi.org/10.1038/nn.2234
126. Raimondi F, Seeber M, Benedetti PG, Fanelli F (2008) Mechanisms of inter- and intramolecular communication in GPCRs and G proteins. J Am Chem Soc 130:4310–4325. https://doi.org/10.1021/ja077268b
127. Rakoczy EP, Kiel C, McKeone R, Stricher F, Serrano L (2010) Analysis of disease-linked rhodopsin mutations based on structure, function, and protein stability calculations. J Mol Biol 405:584–606. https://doi.org/10.1016/j.jmb.2010.11.003
128. Rao VR, Cohen GB, Oprian DD (1994) Rhodopsin mutation G90D and a molecular mechanism for congenital night blindness. Nature 367:639–642. https://doi.org/10.1038/367639a0
129. Rasmussen SG, Devree BT, Zou Y, Kruse AC, Chung KY, Kobilka TS, Thian FS, Chae PS, Pardon E, Calinski D, Mathiesen JM, Shah ST, Lyons JA, Caffrey M, Gellman SH, Steyaert J, Skiniotis G, Weis WI, Sunahara RK, Kobilka BK (2011) Crystal structure of the beta(2) adrenergic receptor-Gs

protein complex. Nature 469:175–181. https://doi.org/10.1038/nature10361
130. Reeves PJ, Hwa J, Khorana HG (1999) Structure and function in rhodopsin: kinetic studies of retinal binding to purified opsin mutants in defined phospholipid-detergent mixtures serve as probes of the retinal binding pocket. Proc Natl Acad Sci U S A 96:1927–1931
131. Richards JE, Scott KM, Sieving PA (1995) Disruption of conserved rhodopsin disulfide bond by Cys187Tyr mutation causes early and severe autosomal dominant retinitis pigmentosa. Ophthalmology 102:669–677
132. Ritter E, Zimmermann K, Heck M, Hofmann KP, Bartl FJ (2004) Transition of rhodopsin into the active metarhodopsin II state opens a new light-induced pathway linked to Schiff base isomerization. J Biol Chem 279:48102–48111
133. Ruprecht JJ, Mielke T, Vogel R, Villa C, Schertler GF (2004) Electron crystallography reveals the structure of metarhodopsin I. EMBO J 23:3609–3620
134. Sakami S, Maeda T, Bereta G, Okano K, Golczak M, Sumaroka A, Roman AJ, Cideciyan AV, Jacobson SG, Palczewski K (2011) Probing mechanisms of photoreceptor degeneration in a new mouse model of the common form of autosomal dominant retinitis pigmentosa due to P23H opsin mutations. J Biol Chem 286:10551–10567. https://doi.org/10.1074/jbc.M110.209759
135. Salom D, Lodowski DT, Stenkamp RE, Le Trong I, Golczak M, Jastrzebska B, Harris T, Ballesteros JA, Palczewski K (2006) Crystal structure of a photoactivated deprotonated intermediate of rhodopsin. Proc Natl Acad Sci U S A 103:16123–16128
136. Sandberg MN, Amora TL, Ramos LS, Chen MH, Knox BE, Birge RR (2011) Glutamic acid 181 is negatively charged in the bathorhodopsin photointermediate of visual rhodopsin. J Am Chem Soc 133:2808–2811. https://doi.org/10.1021/ja1094183
137. Sanders CR, Myers JK (2004) Disease-related misassembly of membrane proteins. Annu Rev Biophys Biomol Struct 33:25–51. https://doi.org/10.1146/annurev.biophys.33.110502.140348
138. Sato K, Morizumi T, Yamashita T, Shichida Y (2010) Direct observation of the pH-dependent equilibrium between metarhodopsins I and II and the pH-independent interaction of metarhodopsin II with transducin C-terminal peptide. Biochemistry 49:736–741. https://doi.org/10.1021/bi9018412
139. Schadel SA, Heck M, Maretzki D, Filipek S, Teller DC, Palczewski K, Hofmann KP (2003) Ligand channeling within a G-protein-coupled receptor. The entry and exit of retinals in native opsin. J Biol Chem 278:24896–24903
140. Scheerer P, Heck M, Goede A, Park JH, Choe HW, Ernst OP, Hofmann KP, Hildebrand PW (2009) Structural and kinetic modeling of an activating helix switch in the rhodopsin-transducin interface. Proc Natl Acad Sci U S A 106:10660–10665. https://doi.org/10.1073/pnas.0900072106
141. Scheerer P, Park JH, Hildebrand PW, Kim YJ, Krauss N, Choe HW, Hofmann KP, Ernst OP (2008) Crystal structure of opsin in its G-protein-interacting conformation. Nature 455:497–502. https://doi.org/10.1038/nature07330
142. Scheerer P, Sommer ME (2017) Structural mechanism of arrestin activation. Curr Opin Struct Biol 45:160–169. https://doi.org/10.1016/j.sbi.2017.05.001
143. Shenker A (1995) G protein-coupled receptor structure and function: the impact of disease-causing mutations. Bailliere Clin Endocrinol Metab 9:427–451
144. Sieving PA, Fowler ML, Bush RA, Machida S, Calvert PD, Green DG, Makino CL, McHenry CL (2001) Constitutive "light" adaptation in rods from G90D rhodopsin: a mechanism for human congenital nightblindness without rod cell loss. J Neurosci 21:5449–5460
145. Sieving PA, Richards JE, Naarendorp F, Bingham EL, Scott K, Alpern M (1995) Dark-light: model for nightblindness from the human rhodopsin Gly-90–>Asp mutation. Proc Natl Acad Sci U S A 92:880–884. https://doi.org/10.1073/pnas.92.3.880
146. Singhal A, Guo Y, Matkovic M, Schertler G, Deupi X, Yan EC, Standfuss J (2016) Structural role of the T94I rhodopsin mutation in congenital stationary night blindness. EMBO Rep 17:1431–1440. https://doi.org/10.15252/embr.201642671
147. Singhal A, Ostermaier MK, Vishnivetskiy SA, Panneels V, Homan KT, Tesmer JJ, Veprintsev D, Deupi X, Gurevich VV, Schertler GF, Standfuss J (2013) Insights into congenital stationary night blindness based on the structure of G90D rhodopsin. EMBO Rep. https://doi.org/10.1038/embor.2013.44
148. Standfuss J, Edwards PC, D'Antona A, Fransen M, Xie G, Oprian DD, Schertler GF (2011) The structural basis of agonist-induced activation in constitutively active rhodopsin. Nature 471:656–660. https://doi.org/10.1038/nature09795
149. Standfuss J, Xie G, Edwards PC, Burghammer M, Oprian DD, Schertler GF (2007) Crystal structure of a thermally stable rhodopsin mutant. J Mol Biol 372:1179–1188. https://doi.org/10.1016/j.jmb.2007.03.007
150. Stenkamp RE (2008) Alternative models for two crystal structures of bovine rhodopsin. Acta Crystallogr D Biol Crystallogr D64:902–904. https://doi.org/10.1107/S0907444908017162
151. Stojanovic A, Hwang I, Khorana HG, Hwa J (2003) Retinitis pigmentosa rhodopsin mutations L125R and A164V perturb critical interhelical interactions: new insights through compensatory mutations and crystal structure analysis. J Biol Chem 278:39020–39028. https://doi.org/10.1074/jbc.M303625200
152. Suda K, Filipek S, Palczewski K, Engel A, Fotiadis D (2004) The supramolecular structure of the GPCR rhodopsin in solution and native disc membranes. Mol Membr Biol 21:435–446
153. Sun D, Flock T, Deupi X, Maeda S, Matkovic M, Mendieta S, Mayer D, Dawson RJ, Schertler GF, Babu MM, Veprintsev DB (2015) Probing Galphai1 protein activation at single-amino acid resolution. Nat Struct Mol Biol 22:686–694. https://doi.org/10.1038/nsmb.3070
154. Sung CH, Davenport CM, Nathans J (1993) Rhodopsin mutations responsible for autosomal dominant retinitis pigmentosa. Clustering of functional classes along the polypeptide chain. J Biol Chem 268:26645–26649
155. Sung CH, Schneider BG, Agarwal N, Papermaster DS, Nathans J (1991) Functional heterogeneity of mutant rhodopsins responsible for autosomal dominant retinitis pigmentosa. Proc Natl Acad Sci U S A 88:8840–8844
156. Szczepek M, Beyriere F, Hofmann KP, Elgeti M, Kazmin R, Rose A, Bartl FJ, von Stetten D, Heck M, Sommer ME, Hildebrand PW, Scheerer P (2014) Crystal structure of a common GPCR-binding interface for G protein and arrestin. Nat Commun 5:4801. https://doi.org/10.1038/ncomms5801
157. Tam BM, Moritz OL (2009) The role of rhodopsin glycosylation in protein folding, trafficking, and light-sensitive retinal degeneration. J Neurosci 29:15145–15154. https://doi.org/10.1523/JNEUROSCI.4259-09.2009
158. Tao YX (2008) Constitutive activation of G protein-coupled receptors and diseases: insights into mechanisms of activation and therapeutics. Pharmacol Ther 120:129–148. https://doi.org/10.1016/j.pharmthera.2008.07.005
159. Teller DC, Okada T, Behnke CA, Palczewski K, Stenkamp RE (2001) Advances in determination of a high-resolution three-dimensional structure of rhodopsin, a model of G-protein-coupled receptors (GPCRs). Biochemistry 40:7761–7772
160. Themmen AP, Martens JW, Brunner HG (1998) Activating and inactivating mutations in LH receptors. Mol Cell Endocrinol 145:137–142
161. Tsai CJ, Marino J, Adaixo R, Pamula F, Muehle J, Maeda S, Flock T, Taylor NM, Mohammed I, Matile H, Dawson RJ, Deupi X, Stahlberg H, Schertler G (2019) Cryo-EM structure of the

rhodopsin-Galphai-betagamma complex reveals binding of the rhodopsin C-terminal tail to the gbeta subunit. Elife 8. https://doi.org/10.7554/eLife.46041
162. Tsai CJ, Pamula F, Nehme R, Muhle J, Weinert T, Flock T, Nogly P, Edwards PC, Carpenter B, Gruhl T, Ma P, Deupi X, Standfuss J, Tate CG, Schertler GFX (2018) Crystal structure of rhodopsin in complex with a mini-Go sheds light on the principles of G protein selectivity. Sci Adv 4:eaat7052. https://doi.org/10.1126/sciadv.aat7052
163. Van Eps N, Preininger AM, Alexander N, Kaya AI, Meier S, Meiler J, Hamm HE, Hubbell WL (2011) Interaction of a G protein with an activated receptor opens the interdomain interface in the alpha subunit. Proc Natl Acad Sci U S A 108:9420–9424. https://doi.org/10.1073/pnas.1105810108
164. Vishveshwara S, Ghosh A, Hansia P (2009) Intra and intermolecular communications through protein structure network. Curr Protein Pept Sci 10:146–160
165. Wittinghofer A, Vetter IR (2011) Structure-function relationships of the G domain, a canonical switch motif. Annu Rev Biochem 80:943–971. https://doi.org/10.1146/annurev-biochem-062708-134043
166. Yan EC, Kazmi MA, De S, Chang BS, Seibert C, Marin EP, Mathies RA, Sakmar TP (2002) Function of extracellular loop 2 in rhodopsin: glutamic acid 181 modulates stability and absorption wavelength of metarhodopsin II. Biochemistry 41:3620–3627
167. Yan EC, Kazmi MA, Ganim Z, Hou JM, Pan D, Chang BS, Sakmar TP, Mathies RA (2003) Retinal counterion switch in the photoactivation of the G protein-coupled receptor rhodopsin. Proc Natl Acad Sci U S A 100:9262–9267
168. Zhang M, Wang W (2003) Organization of signaling complexes by PDZ-domain scaffold proteins. Acc Chem Res 36:530–538
169. Zhao DY, Poge M, Morizumi T, Gulati S, Van Eps N, Zhang J, Miszta P, Filipek S, Mahamid J, Plitzko JM, Baumeister W, Ernst OP, Palczewski K (2019) Cryo-EM structure of the native rhodopsin dimer in nanodiscs. J Biol Chem 294:14215–14230. https://doi.org/10.1074/jbc.RA119.010089
170. Zhou XE, Gao X, Barty A, Kang YY, He YZ, Liu W, Ishchenko A, White TA, Yefanov O, Han GW, Xu QP, de Waal PW, Suino-Powell KM, Boutet S, Williams GJ, Wang MT, Li DF, Caffrey M, Chapman HN, Spence JCH, Fromme P, Weierstall U, Stevens RC, Cherezov V, Melcher K, Xu HE (2016) X-ray laser diffraction for structure determination of the rhodopsin-arrestin complex. Sci Data 3:160021. https://doi.org/10.1038/Sdata.2016.21
171. Zhou XE, He YZ, de Waal PW, Gao X, Kang YY, Van Eps N, Yin YT, Pal K, Goswami D, White TA, Barty A, Latorraca NR, Chapman HN, Hubbell WL, Dror RO, Stevens RC, Cherezov V, Gurevich VV, Griffin PR, Ernst OP, Melcher K, Xu HE (2017) Identification of phosphorylation codes for arrestin recruitment by G protein-coupled receptors. Cell 170:457–469. https://doi.org/10.1016/j.cell.2017.07.002